91602
new 82-10

LEGAL NOTICE

This report was prepared by Ontario Hydro and, while effort has been made to assure the accuracy and applicability of the material contained herein, neither Ontario Hydro nor any person acting on its behalf:

(a) makes any warranty, express or implied with respect to the use of any information, apparatus, method or process disclosed in this report or that such use may not infringe privately owned rights; or

(b) assumes any liabilities with respect to the use of, or for damages resulting from the use of, any information, apparatus, method or process disclosed in this report.

ontario hydro
research division

COMPLIMENTARY COPY
Please Credit Ontario Hydro Research if Reproduced in Whole or in Part

MATERIALS INTEGRITY SECTION
A REVIEW OF 1988 AND PROPOSALS FOR 1989

Report No 89-141-K

R.G. Fleck
Supervising Engineer
Materials Integrity Section
Metallurgical Research Department

ABSTRACT

This report describes the work programs performed in 1988 by the Materials Integrity Section of the Metallurgical Research Department. The direction of the 1989 work programs is outlined.

job	file	date	report no.
84-875-0200	823.1	June 19, 1989	89-141-K

91602
new 82-10

ontario hydro
research division

EXECUTIVE SUMMARY

MATERIALS INTEGRITY SECTION: A REVIEW OF 1988 AND PROPOSALS FOR 1989

R.G. Fleck

In 1988 the Materials Integrity Section continued with studies in support of CANDU fuel channels. The programs were in the areas of: Fracture Mechanisms and Deformation Mechanisms. Studies were also performed in support of thermal plant operation and secondary side components in nuclear plant.

Fracture Mechanisms studies concentrated on the effects of hydrides on the integrity of pressure tubes. The research programs investigate the parameters that influence: blister formation, the initiation of delayed hydride cracks (DHC) from cracked blisters, DHC initiation in rolled joint assemblies and test specimens and DHC growth with emphasis on the tunnelling aspects of such cracks. Development continued on the technique to nondestructively measure hydrogen in pressure tubes.

Deformation Mechanisms studies concentrated on analysis of reactor measurement data and modifications to the CDEPTH code to predict fuel channel sag and pressure tube/calandria tube contact. The high flux experiment in Dido continued and illustrated that the temperature dependence of growth for Zr-2.5 Nb is opposite to that for Zircaloy. Transmission electron microscopy on irradiated material indicates that dislocations are introduced by the irradiation damage and that phase changes also occur. The production of TG3-R1 pressure tubes resulted in a high incidence of cracking in the cold draw stage. Metallurgical evaluation indicates no difference in the properties between the 1988 material and the original development material. Modifications to the design of the cold draw dies has been recommended and will be used on a limited number of tubes.

In support of thermal plant a facility for the creep testing of non-standard specimens has been developed. The loop for corrosion/fatigue tests is complete and initial tests have been performed.

To maintain some expertise in fuel clad metallurgy, a program on the oxidation and biaxial deformation is underway. The program relates to the exposure of cladding to degraded cooling conditions and generates information on oxidation rates in air and steam and the mechanical properties of oxidized cladding to assess integrity under postulated handling incidents.

job	file	date	report no.
84-875-0200	823.1	June 19, 1989	89-141-K

TABLE OF CONTENTS

		Page
1.0	INTRODUCTION	1
2.0	MATERIALS INTEGRITY SECTION PERSONNEL	2
3.0	FRACTURE MECHANISMS UNIT - 1988 REVIEW	3
3.1	Blisters	3
3.1.1	Deuterium Ingress Task Group (DITG)	3
3.1.2	Crack Initiation and Growth from Hydride Blisters	4
3.1.3	Probabilistic Modelling of Tube Fracture Due to Blisters for Reactor Assessment	5
3.2	Development of a Technique for the Nondestructive Evaluation of Hydrogen in Zirconium Pressure Tube Material	6
3.3	Delayed Hydride Crack Initiation	7
3.3.1	Rolled Joint Integrity	7
3.3.2	Delayed Hydride Cracking and Fatigue	8
3.3.3	Crack Initiation in Pressure Tube Materials	9
3.4	Delayed Hydride Crack Growth Studies	10
3.4.1	Evaluation of Yttrium Sink Encapsulation	17
3.5	Thermal Cycling on Hydride Orientation	17
3.6	Hydriding of Pressure Tube Samples	19
3.7	EPRI Project No. RP1890-5: Corrosion Fatigue Boiler Tube Failure in Waterwalls and Economizers	19
3.7.1	Technical Approach	19
3.7.2	Development of Equipment and Test Procedure	19
3.7.2.1	Flow Loop and Test Facility Developments	19
3.7.3	Test Procedure Developments	21
3.7.3.1	Essentials of the Test Procedure Developed	21
3.7.3.2	Main Experimental Accomplishments in Tube Testing	21
4.0	DEFORMATION MECHANISMS UNIT - 1988 REVIEW	23
4.1	Reactor Data Analysis	23
4.1.1	Modifications to CDEPTH	23
4.1.2	Deformation Database	24
4.1.3	Contact Spreading Model	25
4.1.3.1	Refinement of the Model	25
4.1.4	Comparison of Contact Spreading Rates in Pickering-A and Bruce-A	28
4.1.5	Study of the Effect of Channel Power on Contact Spreading Rates	28
4.1.6	Derivation of New Calandria Tube Creep Constant for Bruce-A	29

TABLE OF CONTENTS (Cont'd)

		Page
4.2	Fuel Channel Maintenance Support	29
	4.2.1 Pinching of Channel Spacers in PNGS-A and BNGS-B	29
	4.2.2 Range of Sag in P3/P4 at Time of Scheduled LSFCR	30
	4.2.3 Assessment of Mock-Up Fuel Channels in SLAR Test Rig	30
	4.2.4 Other Reactor Maintenance Support	31
	4.2.5 Contact Predictions for Point LePreau Fuel Channels	31
4.3	In-Reactor Deformation Mechanisms	31
	4.3.1 Dido Program	31
	4.3.2 Characterization of Irradiation	35
	4.3.3 Osiris Program	37
	4.3.4 Evaluation of Power Reactor Fast Fluxes	37
4.4	The β to α Transformation in a Zr-2.5 Wt% Nb Alloy	39
4.5	C-Component Dislocations in Sub-Boundaries in a Zr-2.5 Wt% Nb Alloy	39
	4.5.1 Tilt Boundaries	39
	4.5.2 Twist Boundaries	39
4.6	Pressure Tube Development	40
4.7	Tensile Evaluation of TG3 R1 Tubes	42
4.8	Tensile Properties of Zr-2.5 Wt% Nb Pressure Tube Materials Under High Applied Strain Rate Conditions	42
4.9	Steam Oxidation, Biaxial Deformation and Beryllium-Assisted Crack Penetration Behaviour of CANDU Reactor Zircaloy-4 Fuel Cladding at Elevated Temperatures	45
	4.9.1 Steam Oxidation Kinetics	45
	4.9.2 Biaxial Deformation Behaviour in Air	48
	4.9.3 Beryllium-Assisted Crack Penetration Behaviour at Elevated Temperatures	48
4.10	Miscellaneous Tensile Testing Using the Computer-Controlled Materials Characterization Test Facility	48
4.11	Tensile Properties of Darlington PHT Piping Materials	50
4.12	Method to Initiate ID Cracks in Zr-2.5 Wt% Nb Pressure Tube Samples	50
4.13	Inert Atmosphere Testing of Thermal Plant Materials	51
5.0	SEM PROGRAMS	51
		55
1989 PROGRAMS		
6.0	FRACTURE MECHANISMS UNIT	55
6.1	Blisters	55
	6.1.1 Probabilistic Modelling of Tube Fracture Due to Blisters for Reactor Assessment	55

TABLE OF CONTENTS (Cont'd)

		Page
	6.1.2 Crack Initiation and Growth from Hydride Blisters	56
	6.1.3 Crack Initiation	56
	6.1.4 Crack Growth	56
6.2	Hydride Morphology	56
6.3	Nondestructive Evaluation of Hydrogen in Pressure Tubes	57
	6.3.1 Proposal for 1989/90	57
6.4	Corrosion Fatigue Boiler Tube Failures in Waterwalls and Economizers - EPRI Project RP1890-5	57
7.0	DEFORMATION MECHANISMS UNIT	57
7.1	Analysis of In-Service Deformation Behaviour of Fuel Channels	57
7.2	High Fluence Irradiation Effects in Zr-2.5 Nb Pressure Tubes	57
7.3	Evaluation of Power Reactor Fast Fluxes	58
7.4	Advanced Carrier Bundle	58
7.5	Fuel Clad Oxidation	59
7.6	Pressure Tube Development	59
7.7	Support for Thermal Plants	59
8.0	SEM PROGRAMS	60
REPORTS		61
PRESENTATIONS/PUBLICATIONS		63
CONFERENCES AND TECHNICAL MEETINGS		64
DISTRIBUTION		Last page

ontario hydro
research division

TO: D. Mills
Director of Research

MATERIALS INTEGRITY SECTION
A REVIEW OF 1988 AND PROPOSALS FOR 1989

1.0 INTRODUCTION

The work programs of the Materials Integrity Section are mainly funded by the CANDU Owners Group (COG). This necessitates the co-ordination of our programs with those at AECL-RC and the fuel channel research is planned over a five year period. The progress of the COG funded programs is reported quarterly and this annual report is prepared to coincide with the March 31st COG year-end.

Pressure tubes continue to be the main area of research for the Materials Integrity Section with studies on Fracture Mechanisms and Deformation Mechanisms. The programs in each of these areas are as follows: i) Fracture Mechanisms considers the metallurgical and operating parameters that control blister formation and cracking, the initiation and growth of delayed hydride cracking (DHC). As a result of the concerns with the precipitation of hydrides in zirconium alloys an initiative was taken to develop a technique to non-destructively measure the hydrogen content of pressure tube alloys. This technique was refined in 1988 so that its' subsequent use on irradiated material, which necessitates remote application of the technique, would not be limited by electrical noise problems which would mask the measurement signal. ii) Deformation Mechanisms considers the analysis of in-service deformation measurements on fuel channels with particular emphasis on pressure tube/calandria tube contact predictions. The studies involved the use of and modifications to CDEPTH which were performed in conjunction with staff of the Mechanical Research Department. High flux irradiation programs in Dido were continued and specimens prepared from a surveillance pressure tube were included. Extensive preparatory work was performed for the start of the irradiation creep and growth program in the Osiris reactor at Saclay, France. Investigation of the occurrence of cracks in the production of TG3-R1 pressure tubes was performed with the emphasis on comparing the properties of the 1988 material with those of the material used in the original 1980 trial production.

With the above two areas of study in the same Section easy interaction of ideas occurred which resulted in cooperative efforts in the development of the probabilistic model used to assess the reliability of pressure tubes with respect to blister formation.

Although the major bulk of the work is in pressure tubes, programs in other areas are also performed. Support to thermal plant problems is provided on a limited scale due to resource restrictions. These studies are mainly on corrosion/fatigue which is supported by EPRI. Other areas of research are related to the evaluation of the mechanical properties of fuel clad exposed to degraded cooling conditions and the determination of the mechanical properties of materials used in the secondary side of the CANDU system. The work programs in each of the above areas are presented in this report.

Fundamental to the studies of the Materials Integrity Section are capabilities to evaluate the detailed microstructure of the pressure tube alloys. To provide this information the Section has expertise in the areas of transmission electron microscopy (TEM) and X-ray diffraction. The TEM capabilities have been increased with the examination of irradiated material. Specimens from surveillance pressure tubes and from Dido growth specimens have been examined on the TEM at OHRD. Despite the limited capabilities of the instrument some important and detailed studies have been performed. For 1989 it is a priority of the Section to gain access to a state-of-the-art analytical TEM.

The responsibilities of the Section were increased in 1988 to include the JEOL 840A scanning electron microscope (SEM). The main objectives were to increase the use of the SEM in longer term projects that required the resolution and analytical capabilities of the instrument. This resulted in a decrease in the use of the SEM for short-term service oriented work and for 1988 the main programs were in the area of corrosion in support of studies in the Metallurgical and Chemical Research Departments.

2.0 MATERIALS INTEGRITY SECTION PERSONNEL

R.G. Fleck	Supervising Engineer
L.J. Compton	Section Secretary
E.T.C. Ho	Engineer (Technical Side of Dual Ladder)
S. Sandloehken	Technician - SEM
M. Leger	Unit Head - Fracture Mechanisms
W. Lee	Engineer
G. Shek	Engineer
K. Tashiro	Engineer
R. Irwin	Technician
O. Kiir	Technologist
D. Oad	Technician
H. Seahra	Technician
P. Vesely	Technologist

R.A. Holt	Unit Head - Deformation Mechanisms
N. Badie	Engineer
V. Perovic	Engineer
A. Donner	Technologist
Z. Grozdanovski	Technologist
R. Jarochowicz	Technician - Electron Optics
M. McGraw	Technologist
A. McMillan	Technician

Summer Students

Miss S. Unterbergs
Mr. J. Peric

Attached Staff

Consultant Dr. D.V. Leemans
(Cross Currents Research and
Policy Consulting Ltd)

3.0 FRACTURE MECHANISMS UNIT - 1988 REVIEW

3.1 Blisters

3.1.1 Deuterium Ingress Task Group (DITG)
(M. Leger)

Support for the work of the DITG was provided in the form of assessments of reactor core pressure tubes using the probabilistic model for blisters developed at OHRD. Several different assessments were carried out during the year. These were:

1. An initial assessment of Pickering Unit 4 using the results of the initial tube microsampling campaign carried out in December 1987.

2. An assessment of Bruce Unit 3 following the microsampling carried out in that reactor. An initial assessment of Bruce Unit 2 using the Unit 3 results was also provided.

3. A reassessment of Pickering Unit 4 following the second microsampling in late 1988.

Some program modifications were also made during the year. These included a modification to allow a databased deuterium pickup scenario to be used. At the start of the year, the program allowed only piecewise-linear rates to be modelled through definition of the means and standard deviations of the

primary pickup, the transition time and the secondary pickup rates. These were tied to temperature along the channel. The databased scenario uses the analyzed data from a given channel for a given Monte Carlo realization and allows a choice for the time dependence of the pickup rate (usually linear or quadratic time dependence has been assumed). Since the data can be tied to either temperature or position along the channel, this method allows additional flexibility in the modelling of pickup.

The recent Pickering Unit 4 assessment indicates that the reliability (defined as the probability of having the reactor core free of critically blistered tubes) begins to decrease within the next few years. Depending upon the deuterium ingress scenario chosen, the average expected time for the first critically blistered tube varies upwards from about 18.5 years. Since there is a will to operate the reactor to at least 18 years, the need for definition of the actual deuterium pickup is obvious.

Similarly, long-term projections for the Bruce reactors are subject to large variability depending upon the deuterium ingress assumptions applied.

Due to the significant dependence of the probabilistic assessments on the deuterium ingress scenarios, some effort was made in analyzing the deuterium microsampling results obtained during the year. This work was done in conjunction with the Reliability and Statistics Section of Operations Research. In the case of the P4 resampling, an attempt was made to determine the significance of the position of the tube in the annulus gas sequence and the orientation of the tube in the reactor (East or West inlet end - these could be different because the tubes were all installed in the reactors with the back ends of the tubes at the West side of the reactor). The large variability in the data made it difficult to determine statistical significance at a high confidence level. It appears that both annulus gas position and tube orientation could be significant factors in explaining some of the variation in the deuterium pickup at several axial positions along the tubes.

3.1.2 <u>Crack Initiation and Growth from Hydride Blisters</u>
(M. Leger, W.K. Lee, O. Kiir, P. Vesely and A. MacMillan)

The main objective of the work is to determine criteria for initiation and growth of cracks from blisters to pressure tube rupture.

Equipment for carrying out the blister growth tests on a pressurized tube has been purchased and is in the assembly stage. A decision was taken to construct the test rig in a tube-test cell rather than building a pressure vessel to contain the test.

Large blisters were grown on an unstressed tube using the air-jet technique. Almost all of them were cracked during growth. The tube has been examined ultrasonically and attempts have been made to determine the depths of the cracks in the blisters using crack-tip diffraction techniques. Initial

metallography was completed on two of the inspected blisters. The observed cracks were completely contained within the blister and did not reach the blister boundary.

Further work was carried out to measure the stresses present in the blister and the surrounding material. The hole-drilling technique for residual stress measurement, developed within Ontario Hydro by the Applied Mechanics Section, was applied to three blisters with different profile heights. These results indicated that the surface stresses became less compressive with larger blister size and that there were very large compressive stresses within the blisters (up to 600 MPa). In the matrix below the blister, tensile stresses were observed. These results are in qualitative agreement with the finite element modelling previously carried out.

The effect of stress during growth on the relationship between blister size and the stress required to fracture the blister is not yet understood. The tests which were carried out indicated that blisters grown under tensile stress require higher stresses to fracture in subsequent bend tests than those grown without stress. The stress state in blisters grown under stress must be determined.

To determine how delayed hydride cracking will start from a cracked blister, four point bend crack nucleation tests were set up with potential drop monitoring to detect the onset of DHC cracking from cracks in blisters produced by monotonic loading.

Incremental increases in the applied stress were applied to the specimens until crack initiation. After an initial heat up to 300°C, the specimens were held at 250°C for at least two days prior to removal from the furnace. If no cracking had occurred as shown by the dc potential drop method, the applied load was increased. All four cracked blisters exhibited DHC when the applied K on the existing blister cracks was about 15 MPa $\sqrt{m}$. The stress intensity values were estimated from the assumed profile of the blister and confirmed by post test metallographic examination. These results are similar to those produced at WNRE using blisters of considerably different geometry.

3.1.3 Probabilistic Modelling of Tube Fracture Due to Blisters For Reactor Assessment

(M. Leger/D.V. Leemans)

A more sophisticated model which gives a better estimate of the reliability of the reactor (probability that there are no tubes with critically sized blisters in the whole reactor) was developed for use with two garterspring reactors. It uses all the tube-specific information available (e.g. initial hydrogen content, garterspring positions and deuterium pick-up rate) to make the assessment on a reactor basis rather than on the basis of indistinguishable tubes.

Some initial work in the development of an algorithm for the time to contact in four garterspring units was completed. It was based upon work for the Bruce Unit 3 reactor by the Nuclear Systems Department of Design and Development Division. This new algorithm was used to make an assessment of Bruce 3 following the microsampling for deuterium pickup carried out in the fall of 1988.

The computer programs for assessing two garterspring reactors on an indistinguishable-tube basis were rewritten in order to accommodate all postulated deuterium pickup scenarios for both Pickering and Bruce reactors. This rationalization was necessary in order to avoid inconsistent use of various common subroutines. The program has been given the acronym RABIT (Reactor Assessment for Blisters In Tubes). It has been used in the recent assessment of Pickering Unit 4 following a microsampling campaign.

3.2 Development of a Technique for the Nondestructive Evaluation of Hydrogen in Zirconium Pressure Tube Material

(K. Tashiro and D. Oad)

The objective of this program is to develop a technique for the nondestructive evaluation of hydrogen (deuterium) in zirconium pressure tube material.

The technique being investigated relies on the detection of physical property changes as hydrides are being precipitated or dissolved in the Zr-2.5% Nb material. Hydrogen will influence the physical properties of Zr-2.5% Nb by producing a discontinuity in the temperature dependence of the property. Resistivity is the main property under investigation. Confirmation and calibration of the results obtained by these measurements will be confirmed by independent measurements obtained by calorimetry.

The design and construction of the automated test unit is being performed concurrently with the main research program. The main heater and probe deployment system is complete and ready for preliminary tests. Final probe and heater designs are awaiting confirmation from the test jig experiments.

Experiments have been performed to test various types of removable surface thermocouple probes. The purpose of these tests is the selection of the thermocouple surface probe construction which satisfies two main criteria. The criteria are: a minimum temperature error when compared to a thermocouple welded to the surface and minimal disturbance to the tube section's temperature field.

System tests of the new signal conditioning system and heater power supply are encouraging. Noise generated from the power supply and other external noise source effects experienced in the early tube section measurements have been reduced substantially. Recent tube section tests have utilized removable probes in a special test jig. The probes which contain the tungsten carbide tips have had little difficulty in penetrating the oxide layer of the non-irradiated tube sections.

Preliminary measurements on tube sections have produced a disruptive artifact. This artifact appears in the temperature range of 150°C to 200°C on heating and 100°C to 120°C on cooling. An intensive investigation into the nature and elimination of this artifact is currently being pursued.

The heating and cooling rates used during tests have been limited to less than 10°C/min. This limitation is a result of the excessively long time period required for the data acquisition unit to scan all the required data channels.

The main purpose of the calorimetric study is to provide a calibration base for the resistivity studies in non-irradiated Zr-2.5 Nb material. In general, the hydride dissolution and precipitation behaviour appear similar even though a different physical property is being measured in each case. This similarity will allow calibration of resistivity results by calorimetry by utilizing small samples in place of large tube sections.

Various samples with hydrogen concentrations ranging from 14 ppm to 100 ppm were prepared and analyzed. Their collective results form the TSSd and TSSp diagram for hydrogen in the Zr-2.5 Nb system.

Differential hydrogen concentration measurements between two samples are possible using the calorimetric technique. The level of detection for hydrogen concentration differences is determined by sample masses, overall hydrogen concentration and instrument parameters.

Hydrogen concentrations determined by the vacuum extraction method have been stated to have a 10% error level. However, this error was not fully realized in this investigation. This indicates that a longer term study is required in order to characterize the error in the vacuum extraction method and its effects on calorimetric determinations. This investigation will be far less intensive than this study and will be implemented on the occasional basis. This exercise will add to the accuracy of the calorimetric method.

3.3 Delayed Hydride Crack Initiation
(W.K. Lee and P. Vesely)

3.3.1 Rolled Joint Integrity

This test program examines the behaviour of zero clearance rolled joints with machined defects under simulated reactor operating condition.

Rolled joints with 60 ppm hydrogen were pressurized with nitrogen to 10 MPa and thermally cycled between 300°C and 250°C to promote hydride precipitation. The rolled joint with the weld-on end plug was first hydrostatically proof tested to 10 MPa. To detect the onset of cracking, we used a high temperature Dunegan differential acoustic emission (AE) transducer with adequate sensitivity up to about 200 kHz.

The test has been running for five months with weekly thermal cycling. The acoustic emission system did not detect any delayed hydride cracking. During each thermal cycle the AE equipment registered noise signals, however, at constant temperature there were no AE events.

3.3.2 Delayed Hydride Cracking and Fatigue
(W.K. Lee, P. Vesely, D.A. Scarth, F.W. Kwok)

This project investigates the effect of load following operation on delayed hydride crack initiation. The experimental part examines the notched tensile specimens exposed to cyclic thermal and mechanical loading. The test parameters are: cyclic loading, constant loading, frequency of mechanical loading, notch type, location of notch (ID and OD).

For a typical test, a thermal cycle to 300°C was applied to the notched specimen prior to the fatigue load cycling at 250°C to promote hydride precipitation. Duplicate tests were carried out for each test condition. The first test specimen was normally tested to failure and the repeat specimen was then tested until the first detectable crack was found by dc potential drop.

Fine tuning of the electrical potential drop crack detection technique has resulted in greater sensitivity. The improved method uses the rate of change in the crack voltage to the reference voltage as an indication of the onset of cracking. We can detect crack size down to about 20 μm. The standard method involved only the detection of an increase in the crack/reference ratio.

Initial test results indicated that the cycles to crack initiation depended on the loading ratio (minimum to maximum load), the loading frequency and the presence of hydrogen. Comparisons between the OD and ID specimens (which have different levels of surface residual stresses) showed that there was no significant difference in fatigue life. Radial hydrides were found in the high R ratio test specimens, and the failure times were shorter for high R ratio specimens. The compressive stress field during the low stress part of the cycle in the low R ratio test prevented hydride formation at the notch tip. The longer cycle period test had smaller number of cycles to failure. Under the same test conditions, the hydrided material has a shorter life time than the as received material. The results were also compared with previously reported work on irradiated material. Again the hydrided material showed a marked decrease in fatigue life. In order to have a direct comparison with the irradiated data, additional specimens without hydride were prepared.

For comparison with the fatigue data, a constant load testing system was set up to carry out standard DHC experiment on the notched tensile specimens.

Finite element analysis and Neuber's rule with deformation plasticity were used to estimate the notch tip stress/strain values. The Neuber's rule relates the elastic stress concentration factor to the stress and strain concentration values at the notch tip. Deformation plasticity theory provides

a closed-form solution for the three dimensional stress/strain state at the notch. The strain values obtained from the Neuber's rule were different from the elastic-plastic finite element solution under certain test conditions.

The above analysis suggested that care should be taken in the use of the Neuber's rule for component life prediction. For example, laboratory notched specimen will withstand an applied strain lower than the theoretical value determined through the Neuber's rule. If these laboratory results are used without adjustment for life estimation, nonconservative prediction may result.

3.3.3 Crack Initiation in Pressure Tube Materials
(W.K. Lee, P. Vesely, A.H. Chan)

Studies were performed on three topics to improve the understanding of the crack initiation process in Zr 2.5 wt% Nb material. These were: four point bend crack initiation tests, fitting probability models to experimental data, and a parametric study on notched tensile specimens.

Except for the specimens loaded to 400 MPa, all the other four point bend specimens have not resulted in failure yet. The hydrogen ingress test specimens have about 16000 hours of exposure and the thermally cycled specimens have reached about 600 cycles.

A preliminary sensitivity analysis of a time-independent exponential probability function to describe crack initiation indicated a strong dependence on the threshold stress intensity factor. With K_{IH} as an input variable, we can calculate the applied K value to obtain the desired probability value. The probability curves are very similar to experimental results using K as correlation parameter.

An improved version of the probability model showed a good correlation between the probability of failure and the cycle time for each set of applied stress/depth combination. Since K (a Linear Elastic Fracture Mechanics parameter) cannot be used for all stress states, analysis problems were encountered with the current data being generated by CRNL and CGE. Very high stresses and shallow notches were used in the test specimens. It was found that the combination of applied stress and notch depth was more useful than K for producing a correlation.

To determine the parameters influencing crack initiation, a new program was set up to investigate the effects of variation in strength (standard pressure tube vs tube annealed at 550°C), notch sharpness(sharp vs blunt), hydride length (<50 μm vs >100 μm) and stress level during hydride growth. The following paragraphs summarize the progress.

The critical loading parameters to cause cracking in notched specimens with specific hydride distribution will be measured for correlation with the notch tip stress/strain values. Variation in specimen preparation will define the hydride distribution. For example, a blunt notched specimen will have a

hydride distribution different from that in a sharp notched specimen. We can then determine the parameters that control crack initiation and relate them to service conditions.

The preparation of specimens with about 60ppm hydrogen was completed. The specimens were first loaded to different times to reorient the hydrides to the desired length and distribution. For example, 125 to 175 microns length can be formed under a sharp notch (0.8 mm deep with a root radius of 0.2 mm) when the tensile specimen is loaded to 300 MPa net section stress for 11 days at 250°C. The specimens were quenched to freeze the microstructure and then will be tested in an increasing load tensile machine at 250°C. Except near the specimen surfaces, a fairly even distribution of radial hydrides was present under the machined notch. Figure 1a-1b illustrates the differences in radial hydride distribution. The specimen with a blunt notch (0.8 mm deep with a root radius of 1 mm) was loaded to 380 MPa net section stress for 11 days at 250°C.

The crack detection system using the potential drop technique is being prepared. Since the accurate detection of crack nucleation while the specimen is continuously loaded is critical, an initial trial test with a 1 kHz ac potential drop system was completed with some success. The ac voltage signals changed when the specimen was flexed very slightly, this indicated that the system could respond to deformation. Further comparison with the standard dc method will be necessary. To interface with either a dc or ac potential drop system to detect cracking, a MS-DOS computer together with a HP logger for continuous data acquisition has been selected.

The finite element analysis to determine the notch tip stress/strain values was completed. The notch tip strain values were very uniform throughout the specimen thickness except near the outside surface. The finite element results showed that at the centre of the specimen the 2 D plane strain results were very similar to the 3 D elastic plastic results. The stress/strain results will be used for comparison with the experimental data.

3.4 Delayed Hydride Crack Growth Studies

(G.K. Shek and H. Seahra)

The objectives of this research program are:

1. To evaluate the effects of metallurgical and operating parameters on DHC velocity.

2. To provide more crack growth data on pressure tubes at reactor operating temperature and during thermal cycles.

The following summarizes the work performed in 1988/89:

Crack Tunnelling: A program was initiated to determine the parameters affecting crack tunnelling by DHC and the conditions required to break the surface ligament. The feasibility of using large tensile specimens for the parametric study of crack tunnelling was demonstrated. The tensile specimens

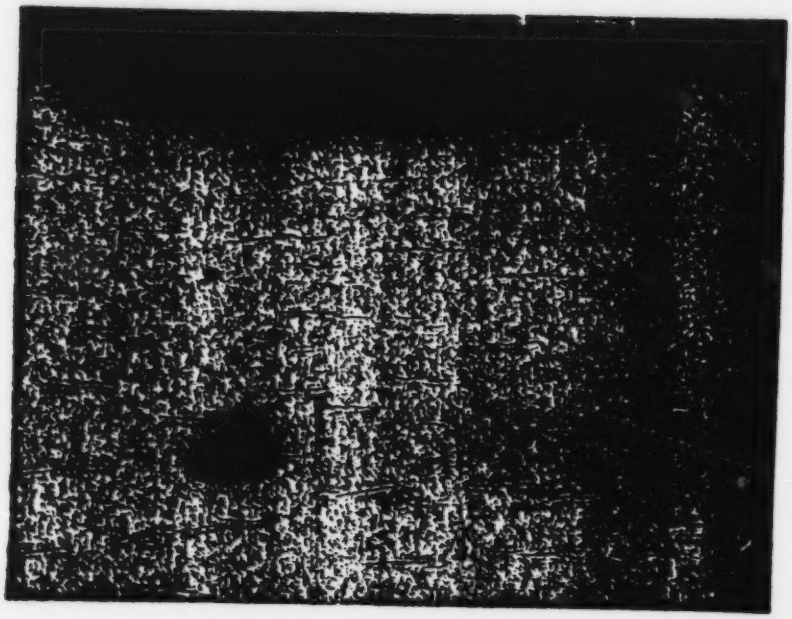

Figure 1a Surface of Specimen 100 X

Figure 1b Mid-section of Specimen 100 X

were machined from strips straightened from pressure tube rings. The loading axis was in the transverse direction of the original tube. In a typical test, DHC was initiated from a semi-elliptical surface notch in a large tensile specimen. Crack initiation and growth was monitored by potential drop. Development of crack shape was marked by thermal or loading cycles. Fractographic and metallographic examination was performed to determine the cracking mechanism and hydride distribution at the crack tip. Figure 2 shows an example of the fracture appearance of one of the test samples. The different stages of crack growth could be clearly distinguished by oxide colour. Test results showed that crack velocities in the axial and radial direction were similar in the initial portion of crack growth. The radial crack velocity was very much reduced when the crack approached the opposite surface, deforming the remaining ligament. However, DHC was able to continue in the radial direction in the deformed ligament for almost the entire wall thickness. Crack growth persisted in a direction perpendicular to the principal tensile stress and did not follow the 45 degree shear band. The crack tunnelled on the notch side as well, leaving behind a deformed surface ligament as the crack advanced in the axial direction. Again, DHC was able to take place in the radial direction in this ligament but at a much reduced rate. By comparing the aspect ratio of the cracks which occurred at different test conditions, it was noted that tunnelling was more extensive for samples cracked at higher stress, probably due to the larger deformed ligament. Difference in cracking temperatures (comparing 200°C to 250°C) appeared to have little effect on the extent of crack tunnelling. Work is underway to design and build a test set-up to determine the effects of temperature gradient through the wall on crack tunnelling.

K Maneuver: An elastic-plastic analysis using the finite element code ABAQUS was performed to determine the stress distribution at the crack tip region of the constant K sample as a result of reduction in K. The calculation showed that compressive residual stress was present at the crack tip as a result of a reduction in K (Figure 3). The nominal tensile stress in the plastic zone was reduced and the maximum tensile stress was further away from the crack tip. In addition, the stress gradient was significantly reduced. The resultant tensile stress depended on the material strength and the conditions of K maneuver (Figure 4). A large embrittled zone at the crack tip (and hence a wider striation) was required for cracking to continue at the lower K level because of the reduction in tensile stress. An incubation period was required to form the larger volume of crack tip hydride under a lower driving force. The effects of K reduction on the calculated maximum tensile stress at the crack tip region, the size of the initial striation spacing and the incubation time are shown in Table 1.

The experimental work was enhanced by the commissioning of two programmable loading frames which allowed automatic load changes according to some preset conditions such as time or crack extension. The K range was expanded from 25-15 to 30-10 $MPa.m^{1/2}$. Test results showed that the incubation time for cracking at 250°C was only about an hour when K was lowered from 30 to

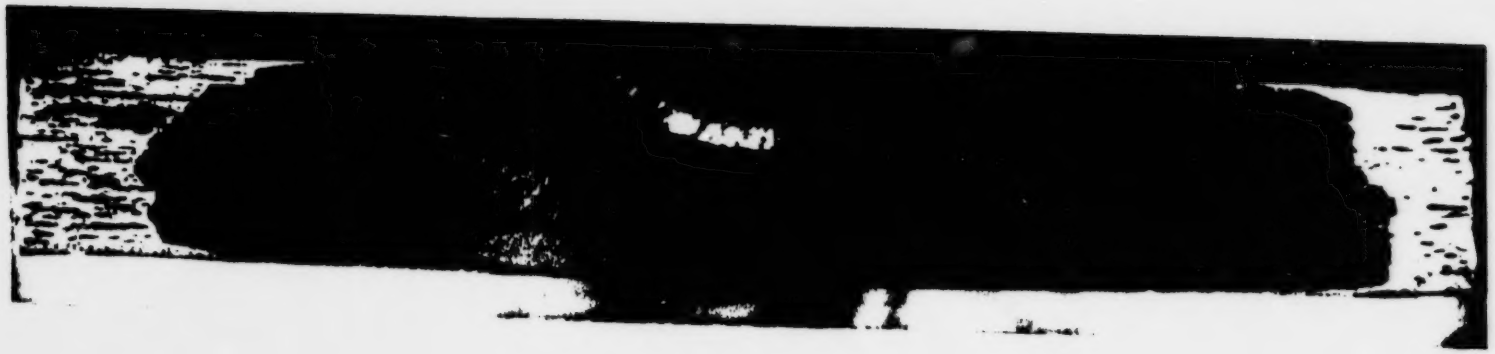

FIGURE 2

Fracture appearance of DHC initiated from a fatigue precracked surface notch in a large tensile sample. Development of crack shape was marked by loading and thermal cycles. ~8X

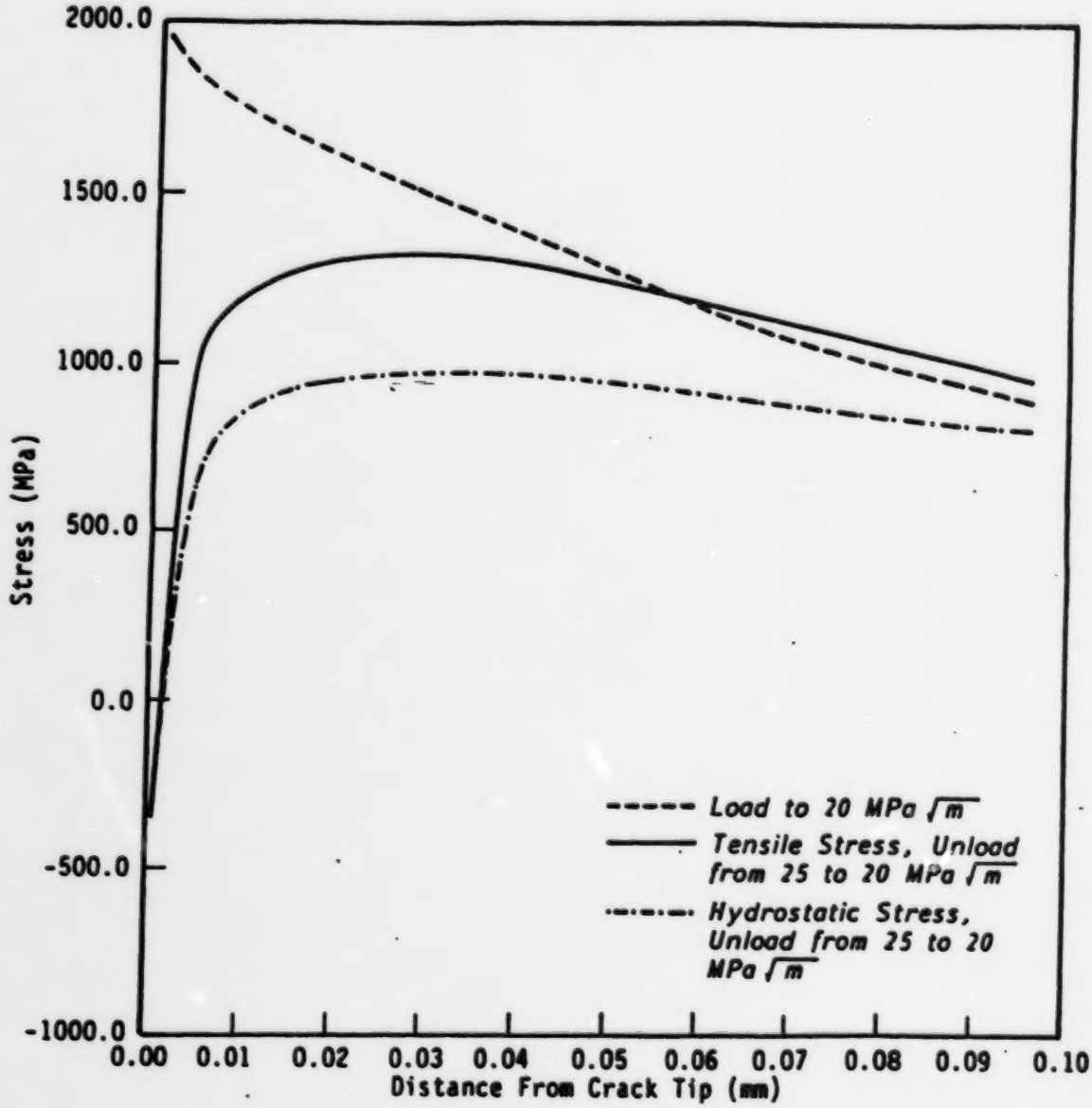

Figure 3 **Effects of K reduction from 25 to 20 MPa.m$^{1/2}$ on the tensile and hydrostatuc stress distribution in the crack tip region determined by finite element analysis.**

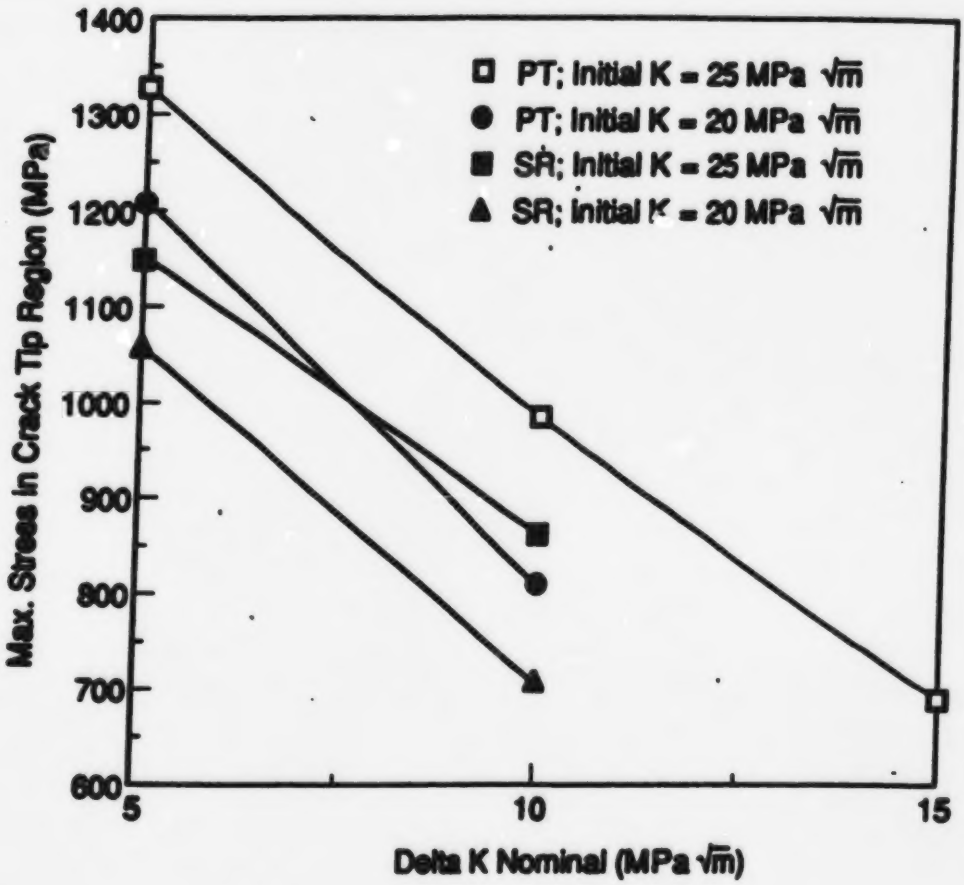

Figure 4 Effects of different K reduction on maximum tensile stress at crack tip region. PT-pressure tube; SR-stress relieved material.

TABLE 1

LENGTH OF INCUBATION TIME AT 250°C AS A FUNCTION OF MAXIMUM TENSILE STRESS CALCULATED FROM THE FINITE ELEMENT ANALYSIS

MATERIAL	ΔK (MPa.$m^{1/2}$)	MAXIMUM TENSILE STRESS (MPa)	INCUBATION TIME	INITIAL STRIATION SPACING (μm)
PT	25→20	1330	1.5-1.7 hrs	59
PT	20→15	1210	4.4 hrs	85
PT	25→15	980	16 hrs	96
PT	25→15	980	No cracking	>108
SR	25→20	1140	24 hrs	220
SR	20→15	1060	No cracking	>166

PT - Zr-2.5 wt % Nb pressure tube material
SR - Pressure tube mat'l, stress relieved

25 MPa.$m^{1/2}$. Cracking stopped and did not resume when K was lowered from 15 to 10 MPa.$m^{1/2}$. These results followed the trend of cracking behaviour observed in previous tests.

Crack re-initiation after K reduction was more difficult as the amount of hydrogen in solution decreased. The effects of amount of hydrogen in solution on cracking behaviour were studied in two ways: (1) by comparing samples with different hydrogen concentrations (40 and 60 ppm hydrogen); (2) by changing the peak temperature in the initial cooling thermal cycle to test temperature. In the latter case, the amount of hydrogen in solution at test temperature increased with higher peak temperature due to TSS hysteresis. The test results showed that crack resumption was more difficult and the incubation time was significantly increased as a result of reduction in hydrogen in solution (Table 2).

3.4.1 Evaluation of Yttrium Sink Encapsulation
(M. Leger)

An evaluation of the potential for DHC in the encapsulating Zircaloy-2 for Yttrium sinks proposed for installation during Pickering retubing was performed at the request of the Yttrium sink technical review committee. The conclusion of the brief review was that there was more than a remote possibility of cracking in the encapsulation. This conclusion was reached by reviewing available information on the stresses, hydrogen levels and laboratory information. The very high, sustained stresses in the encapsulation were thought to be high enough to result in crack initiation in the presence of hydrides at shutdown temperatures. Crack propagation, once initiated could occur during subsequent shut downs.

3.5 Thermal Cycling on Hydride Orientation
(G.K. Shek and H. Seahra)

A co-operative program between CRNL and OHRD has been proposed to irradiate curved compact tension specimens containing "mixed" hydrides so that the combined effects of irradiation and hydride morphology on fracture toughness of pressure tubes can be evaluated. The irradiation temperature will be about 260°C and several thermal cycles may occur during the irradiation period. There is concern that the mixed hydrides may revert to the circumferential orientation as a result of the thermal cycling. A sample containing about 50 ppm mixed hydrides was heated to 262°C, held for four hours and then furnace cooled to 100°C. The thermal cycle was repeated six times. Metallography was performed to compare the hydride morphology before and after the thermal cycling. At low magnification, there was a significant increase in the amount of circumferential hydrides and a noticeable but not drastic reduction of mixed hydrides. At high magnification, it was noted that the mixed hydrides were less continuous after the thermal cycling. It appeared that thermal cycling reduced the thickness and the continuity of the mixed hydrides. It is recommended that samples with higher concentration of mixed hydrides be used for the test program to reduce the effect of thermal cycling on the resultant hydride morphology.

TABLE 2

EFFECTS OF AMOUNT OF HYDROGEN IN SOLUTION ON CRACKING BEHAVIOUR AS A RESULT OF REDUCTION IN STRESS INTENSITY FACTOR

Delta K	Incubation Time (hours)		
(MPa.m1/2)	H conc: 60 ppm Peak Temp: 300°C	H conc: 60 ppm Peak Temp: 270°C	H conc: 40 ppm Peak Temp: 300°C
30 → 25	1 h	4.8 h	≥6.8 h
25 → 20	1.5 h	≥16 h	no cracking
20 → 15	≥2 h	no cracking	---
15 → 10	no cracking	---	---

3.6 Hydriding of Pressure Tube Samples
(G.K. Shek and H. Seahra)

A number of pressure tube samples were hydrided as a service to other Sections by the electrolytic hydriding/diffusion anneal technique to various hydrogen concentration and hydride orientation to support the following programs: measurement of hydrogen concentration by resistivity and eddy current; hydrogen concentration measurements by ultrasound; effects of hydrides and irradiation on fracture toughness; methods of improving leak detection in pressure tubes; effects of internal stresses on hydride precipitation.

3.7 EPRI Project No RP1890-5: Corrosion Fatigue Boiler Tube Failure in Waterwalls and Economizers
(E.T.C. Ho and R.E. Irwin)

To develop a discriminatory laboratory test procedure whereby corrosion fatigue damage representative of that observed in field failures, can be reliably generated under well-controlled test conditions in a section of boiler tubing.

3.7.1 Technical Approach

Analysis of tube failures in the waterwall and economizer regions of boilers, which can be attributed to a corrosion fatigue mechanism, indicates that this type of failure is frequently associated with restraints due to the presence of welded attachments. Such observations indicate that there is a need to establish a correlation between the propensity for cracking and the local design parameters for a given boiler design. To accomplish the above task, the development of a discriminatory laboratory test procedure whereby corrosion fatigue damage representative of that observed in field failures is needed. Since the main features observed in field-generated corrosion fatigue cracks are internal surface initiation and transgranular crack propagation, the required test procedure must be capable of producing these two features in a boiler tube specimen. Specific designs and test parameters to be studied will be based on information obtained from the field monitoring and stress analysis tasks of the overall EPRI-funded project.

3.7.2 Development of Equipment and Test Procedure

3.7.2.1 Flow Loop and Test Facility Developments

The flow loop and the test facility for mechanical cyclic loading of the tube specimens are essentially completed. However, before full testing at high pressures and elevated temperatures can commence, a few trial runs must be carried out to assess the degree of water chemistry control attainable under closed-loop flow conditions at high pressures and elevated temperatures. The main capabilities and operational limits of the test facility and flow loop developed are presented in Table 3.

TABLE 3

SUMMARY OF MAIN CAPABILITIES AND OPERATIONAL LIMITS OF THE FLOW LOOP AND TUBE TEST FACILITY

1. Preheater Output:

   a) 0.17 l/min (2.2 IPG/h) at 325°C and 15 MPa (2200 psi)
   b) higher flow rates possible at lower temperatures and pressures (eg. 0.23 l/min at 250°C and 10 MPa)

2. Feedwater Supply Capacity:

   - 275 l (60 IPG)

3. Load Frame Capacity:

   - ± 250 kN

4. In-line Water Chemistry Monitoring Instrumentation:

   a) dissolved oxygen (upstream and downstream of sample)
   b) pH (upstream and downstream of sample)
   c) conductivity
   d) pressure
   e) temperature (up to 10 channels)
   f) mass flow rate

5. Data Acquisition and Analysis Hardware:

   a) Hewlett Packard VECTRA PC
   b) Hewlett Packard model HP3497A Data Acquisition System

3.7.3 Test Procedure Developments

3.7.3.1 Essentials of the Test Procedure Developed

The test procedure developed utilizes mechanical loading to produce cyclic tensile hoop stresses in the ID surfaces of full size boiler tube specimens. This is accomplished by compressing a plain boiler tube specimen cyclically in a specially-designed loading rig. The design of this loading rig has been described in some detail previously. The test procedure developed has two main features associated with it.

1. The loading rig developed concentrates the cyclic ID surface tensile hoop stresses in a small localized region of a large tube specimen which is typically 30.48 cm (12") long. This localization of deformation means that the site of ID surface crack nucleation can be predetermined within a small region of the specimen. It also means that the required monitoring instrumentation can be deployed efficiently.

2. The testing technique developed utilizes boiler tube material in an unaltered state. This means that the susceptibility of as-manufactured boiler tube material to corrosion fatigue failures can be tested under controlled conditions of water chemistry, temperature, pressure, load amplitude and load frequency.

3.7.3.2 Main Experimental Accomplishments in Tube Testing

To date, several tests have been carried out using boiler tube specimens under both laboratory air and de-ionized water environments at ambient temperature. In the majority of the cases, ID-initiated cracks were produced. The cracks were typically transgranular and non-branched. Both of these features are characteristic of corrosion fatigue cracks observed in the field in boiler tube specimens. A summary of all the tube tests carried out is presented in Table 4.

Results obtained from some metallurgical examinations carried out on the tube specimens indicate that the loading is not uniform axially along the line of contact between the specimen and the lower compression adapter. This arises because when the tube is compressed, it also bends slightly. The axial distribution in loading has been characterized thoroughly. With the MARK II lower compression adapter, the maximum loading is located at about $\pm$30 mm from the midpoint of the line of contact (~75 mm in length). In contrast, with the current lower compression adapter (MARK III), the maximum loading is located at the midpoint of the line of contact (~25 mm in length). Using the MARK III compression adapter, every applied force of 1 kN results in a tensile hoop strain of about 75 $\mu\epsilon$ at the ID surface at the point of maximum loading at ambient temperature.

The flow loop was prepared to produce an initial water chemistry designated as "contaminated AVT water" by B&W in their laboratory crack initiation studies. This water chemistry was specified by B&W as follows:

TABLE 4

Summary of Results for Cyclic Compression Tube Tests

TEST ID	LOAD LIMITS (LOWER ADAPTER)	FREQUENTLY & TOTAL CYCLES	ENVIRONMENT	MAXIMUM DEPTH OF ID CRACK PRODUCED
EPRI.1	6.25-100 kN (MARK I)	1 Hz - 100,000	Laboratory air at ambient temperature	Through wall
EPRI.2	"	1 Hz - 60,000	"	~ 3.0 mm
EPRI.3	"	1 Hz - 40,000	"	0.95 mm
EPRI.4	"	0.017 Hz - 8,000	deionized water at ambient temperature	~ 50 μm
EPRI.30	6.25-100 kN (MARK II)	1 Hz - 25,980	"	2.27 mm
DATAFILE.51	2.5-40 kN (MARK III)	1 Hz - 18,000	laboratory air at ambient temperature	no ID crack found
DATAFILE.52	6.25 - 80 kN (MARK III)	1 Hz - 14,000	"	2.5 mm
DATAFILE.55	2.5 - 40 kN (MARK III)	1 Hz - 80,000	"	1.97 mm
DATAFILE.60	6.25 - 60 kN (MARK III)	1 Hz - 20,000	"	1.62 mm
DATAFILE.65	"	1 Hz - 19,200	de-ionized water at ambient temperature	1.22 mm
DATAFILE.70	6.25 - 100 kN (MARK II)	1 Hz - 25,980	"	2.27 mm

1) chloride (Cl^-) - 600 ppb
2) sulphate ($SO_4^=$) - 600 ppb
3) dissolved oxygen (O_2) - 320 ppb
4) pH (adjusted with ammonia) - 6.5 ± 0.7 units

To achieve the above water chemistry conditions, the flow loop and feedwater tank were cleaned and the feedwater tank was refilled with 250 litres of fresh de-ionized water. Appropriate volumes of stock solutions of sodium chloride (NaCl) and sodium sulphate (Na_2SO_4) were added to the feedwater and allowed to circulate through the closed-loop flow circuit. In addition, pre-purified nitrogen gas with 0.8% oxygen was sparged into the feedwater for approximately 16 h after which time a dissolved oxygen level of 300 ppb was achieved and maintained. Grab samples were obtained for water chemistry analysis. The chemical analyses of the various grab samples taken indicate that the contaminated AVT water chemistry can be maintained at ambient temperature and at 274°C, the desired test temperature.

4.0 DEFORMATION MECHANISMS UNIT - 1988 REVIEW

4.1 Reactor Data Analysis

4.1.1 Modifications to CDEPTH

(N. Badie and R.A. Holt)

A new version of CDEPTH (Version 6) has been issued which includes several modifications and enhancements in order to respond to the increasing requirements of fuel channel sag analysis. The major new features are as follows:

- **New Contact Algorithm**: In order to accommodate axial elongation, which causes large relative motion of the pressure tube with respect to the calandria tube, the contact algorithm has been revised to allow a node on the pressure tube to change its existing relation with nodes on the calandria tube when necessary. A pressure tube node can slide as far as five calandria tube nodes from its original master node. This will increase the stability of the contact algorithm and the accuracy of contact predictions.

- **Curvature Prediction Capability**. This routine computes the pressure tube and calandria tube curvature at each node, and allows a direct comparison to be made between predicted strains and in-reactor measurements.

- **Unloading/Reloading Option on Restart**. Using this option, users can simulate the removal of operating loads and application of the loads experienced during in-reactor measurements. This will allow more accurate comparison of predictions with measurements.

- **SLAR Simulation Option.** This is an extension of the unloading/reloading option, and was developed in response to the growing need for analytical simulation of the Spacer Location and Repositioning operation.

- **New Calandria Tube Design Equation.** The routine which computes the element strain rates has been modified to include the CRNL-4001 calandria tube design equation. The most recent pressure tube/calandria tube design equations (CRNL4000/4001) are now implemented in CDEPTH.

- **Formatted Input File.** The input routine has been changed to accept either free or fixed formatted (rather than list-directed) input. This allows the implementation of error-checking, a limited form of which has been added to the code.

4.1.2 **Deformation Database**
(N. Badie and R.A. Holt)

A study was undertaken to determine whether the fast neutron fluence profiles in the CNS fluence maps for Bruce-A and Pickering-A are derived consistently. This is important when comparing in-reactor deformation data from the two stations. The study focused on the flux profiles in Pickering Unit 3 and Bruce Unit 2 since both operating and inspection data were readily available for these reactors.

The fluence maps for Bruce-A and Pickering-A were found to be inconsistent for three reasons:

- The axially averaged fluences in the CNS fluence maps for Bruce-A reactors are averaged over 13 fuel bundles. However, it takes only 12 bundles to span the reactor core (5.944 m), and the outboard ends of bundles 1 and 13 do not contribute significantly to the fast neutron flux. Therefore, the fluences should be averaged over 12 fuel bundles. Hence the Bruce-A axially averaged fluences should be increased by a factor of 1.083 (ie. 13/12) to be consistent with Pickering-A.

- A consistent set of flux factors have recently been derived for Pickering and Bruce (R.E. Donders, CANDEV 88-58), giving a value of 0.982 for the ratio of the flux factor in Pickering-A to that in Bruce-A. The fluence maps were derived using a ratio of 1.038 between the flux factors. The Bruce-A bundle fluences should therefore be increased by a factor of 1.057 (ie. 1.038/0.982) to remove this inconsistency.

- The sum of the individual channel energy outputs (channel GWh's) over the entire Bruce Unit 2 reactor does not equal the reactor operator's log of reactor energy output (the reactor clock), which is the only reliable record of the total output of the reactor. This inconsistency does not exist in the case of Pickering Unit 3 and Bruce Unit 1. Since

the channel fluences are derived from the channel GWh's, the Bruce Unit 2 fluences should be increased by a factor of 1.06 to be consistent with Pickering-A fluences.

The total effect of these factors is to increase the bundle fluences for Bruce Unit 2 by 12% and the axially averaged fluences by 21% relative to those given in the CNS fluence maps. These corrections have been applied to the CDEPTH calculations used in the fitting of the contact spreading model, and to the sag and contact calculations reported in OHRD Report 88-109-P.

4.1.3 Contact Spreading Model

4.1.3.1 Refinement of the Model

(N. Badie and R.A. Holt)

Work continued on the development of a model for the spreading of contact between the pressure and calandria tubes for the purposes of probabilistic assessment of the reliability of operating reactors. The model has been refined as follows:

- In-reactor inspection data from three Pickering-A channels and one Bruce-A channel have been added to the measured contact database used in fitting the model.

- As a result of the work described below, different spreading rates can now be assigned according to the type of reactor (Pickering-A or Bruce-A) and the power of the channel.

- The "initial spreading" part of the model has been modified, resulting in a much better fit to the CDEPTH results.

- The difference in spreading rate between the inlet and outlet ends of the channel, and between the front and back ends of the pressure tube have been taken into account by adding a new parameter to the model. Another parameter which represents the ratio of the spreading rate towards a channel spacer to the spreading rate towards an end fitting has also been added to the model.

As a result of these changes, the model now gives a significantly better fit to a wider database, while it has become only slightly more complex. (The number of fitted parameters has increased from one to three.) Figure 5 shows the predicted contact spreading curves for three of the channels in the database. The horizontal lines in the figure represent the extent of measured contact. Figure 6 is a graphic comparison of the model's predictions with in-reactor measurements for the nine channels which now form the contact database.

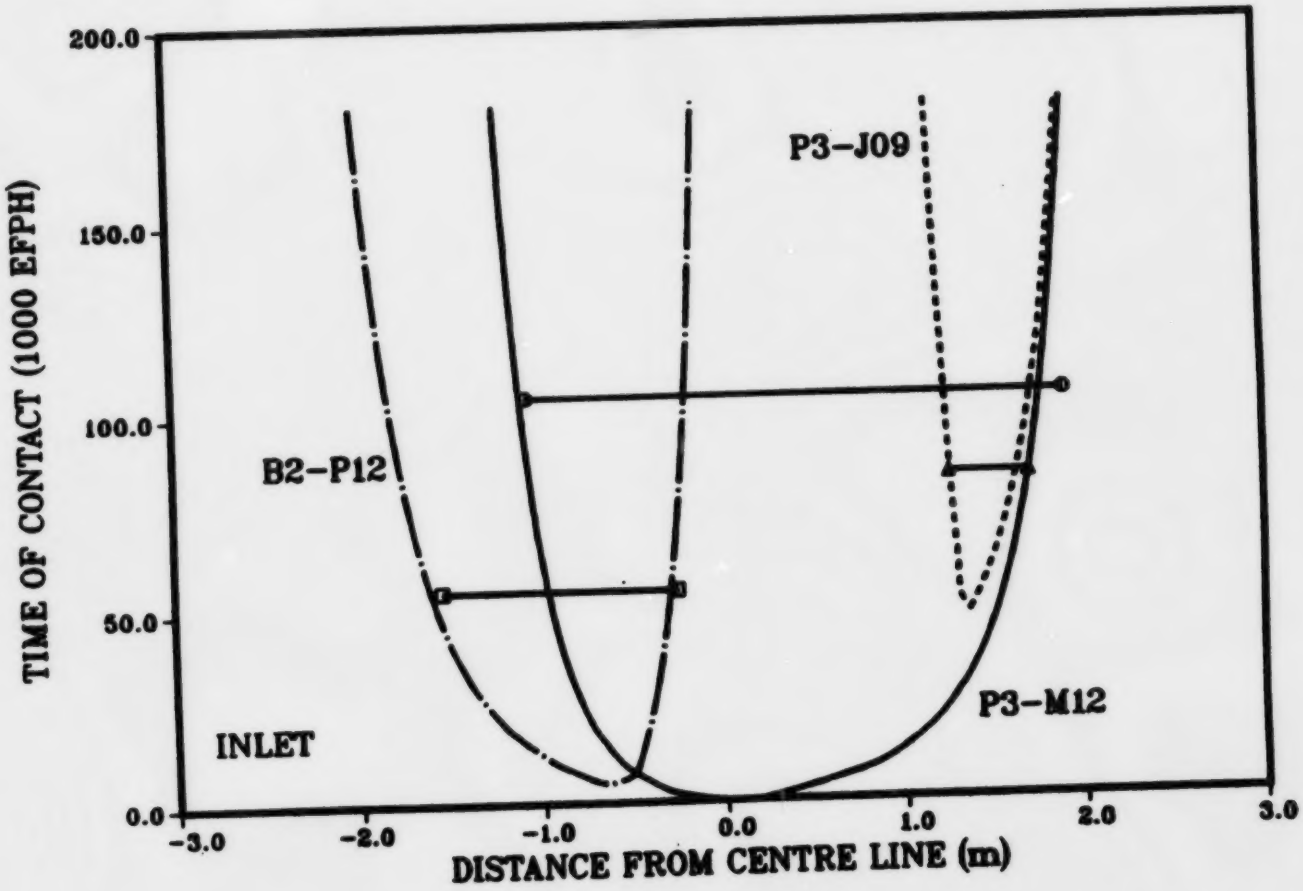

Figure 5: Spreading of Contact in Channels B2–P12, P3–M12 and P3–J09 (Horizontal Lines Represent Measurements)

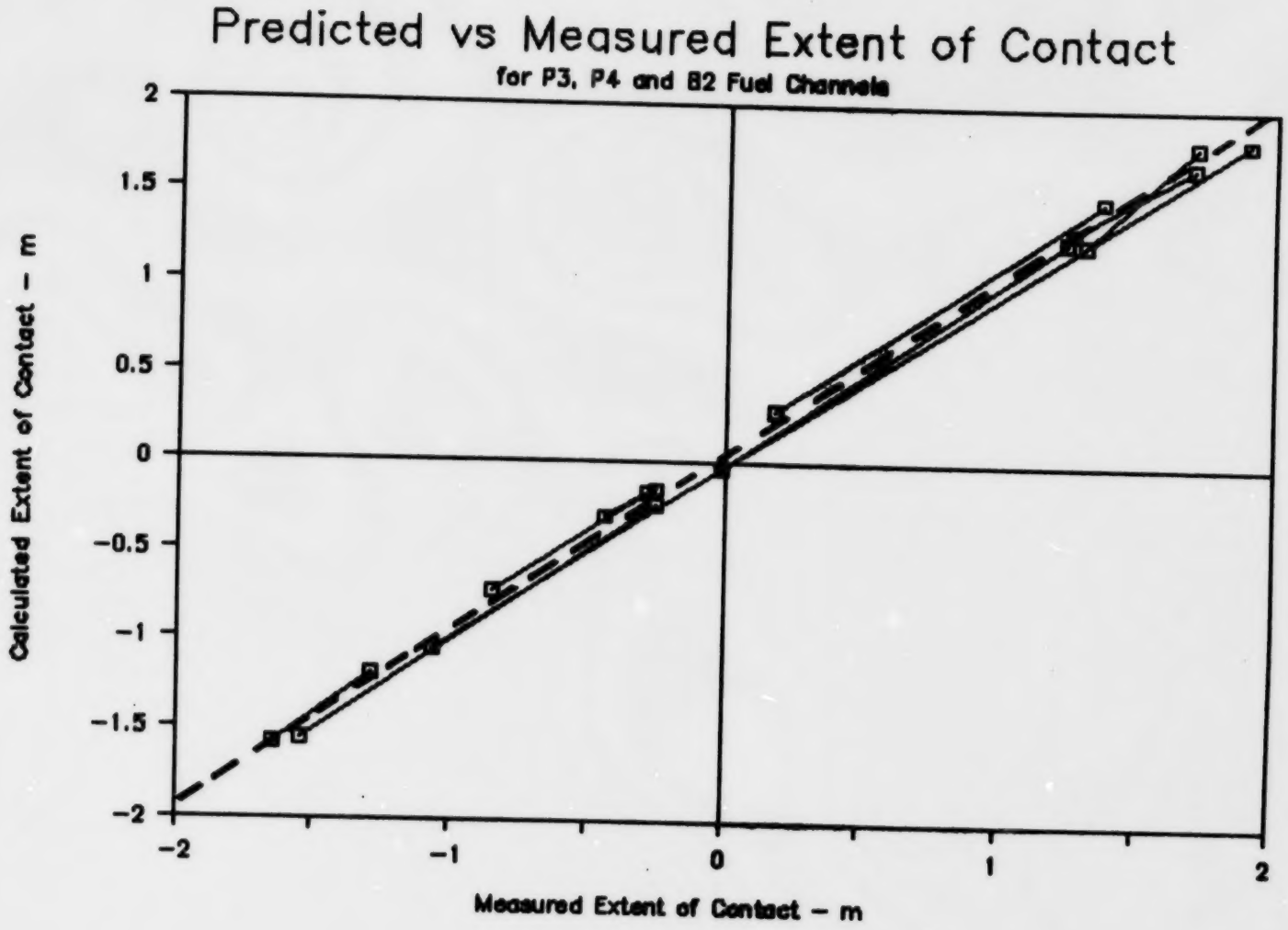
Predicted vs Measured Extent of Contact
for P3, P4 and B2 Fuel Channels
Calculated Extent of Contact – m
Measured Extent of Contact – m
2
1.5
1
0.5
0
-0.5
-1
-1.5
-2
-2
-1
0
1
2

FIGURE 16

The model can be further improved by using the CRNL-4000 design equation for the initial times and locations of contact (a set of nomograms based on CRNL-1993 are used in the current version) and by expanding the database of in-reactor contact measurements.

4.1.4 Comparison of Contact Spreading Rates in Pickering-A and Bruce-A
(N. Badie and R.A. Holt)

This work constitutes the initial part of a study of the effects of channel power, flux and temperature profiles, channel spacer configuration and other operating conditions on the contact spreading rate in CANDU reactors. The results of the study are reported in OHRD Report 88-259-P. These results also formed the data from which the functional form of the contact spreading model was derived.

A set of idealized CDEPTH cases were run with the flux and temperature data representing the average of 16 central channels in Pickering 3 at 100% full power, and in Bruce 2 at 88%, 92% and 100% full power. For the cases studied, the rate of spreading is fastest in Bruce 2 at 100% power, decreases at 92% power, then to 88% power and is slowest in Pickering 3 at 100% power. The long-term spreading rate changes from Bruce 2 at 100% power to 92%, 88% and to Pickering 3 at 100% power in the ratio of 1:0.92:0.87:0.72.

Further, as a result of the study a set of CDEPTH cases were identified which represent the behaviour of fuel channels with different spacer locations. These cases were then used in the study of the effect of channel power on contact spreading rates (see below).

4.1.5 Study of the Effect of Channel Power on Contact Spreading Rates
(N. Badie and R.A. Holt)

The objective of this work is to determine the effect of channel power on the contact spreading rate in Pickering-A and Bruce-A reactors. Initially, the two lowest power channels in Pickering Unit 3 (P3-W08) and Bruce Unit 2 (B2-Y17) were selected and the cases identified in Section 4.1.4 were run in order to compare the contact spreading rates in the channels at both ends of the power spectrum.

The ratio of the P3-W08 channel power to the average power of the 16 central channels of P3 is 0.458, while the ratio of the contact spreading rates between the two is 0.456, indicating that the contact spreading rate varies linearly with channel power. The ratio of B2-Y17 channel power to that of the 16 central channels of B2 is 0.534, while the ratio of the contact spreading rates in this case is 0.576. The dependence of contact spreading rate on channel power again seems close to linear. The slight deviation from linearity is probably due to the higher inlet temperature (approx. 10 K higher) of B2-Y17 (and all outer zone channels) compared with the central channels.

4.1.6 Derivation of New Calandria Tube Creep Constant for Bruce-A
(R.A. Holt and N. Badie)

In the CRNL-1956 calandria tube design equation, the irradiation creep constant of the calandria tube material was given as 4.4×10^{-31} $m^2/n/MPa$. As this number is based on a small database which does not include in-reactor data, a significant uncertainty is associated with it. Given a knowledge of the pressure tube deformation, the calandria tube creep constant can be adjusted to tune the sag deflection predictions to the in-reactor measurements. In this way, in-reactor data will have been included in the derivation of the calandria tube design equation.

The calandria tube creep constant was derived for Pickering-A Units 3&4 and for Bruce-A by fitting the predicted steady state sag rate in P3 and B2 PIP channels, between two fast neutron fluences, to the measured sag rate. The equivalent steady state creep constant for P3 (between 48600 EFPH and 72500 EFPH) is 4.1×10^{-31} $m^2/n/MPa$, and the equivalent steady state creep constant for B2 (between 40600 hours and 61400 hours) is 4.4×10^{-31} $m^2/n/MPa$, giving a ratio of 1.08 between the two equivalent steady state constants. These results were incorporated in the new calandria tube design equation reported in AECL report CRNL-4001.

4.2 Fuel Channel Maintenance Support

4.2.1 Pinching of Channel Spacers in PNGS-B and BNGS-B
(N. Badie and R.A. Holt)

This brief study was carried out in response to a request from Central Production Services to determine the time after which all four garter springs in PNGS-B and BNGS-B would remain pinched between the pressure and calandria tubes even after removal of the fuel for inspection. Their concern was that an early inspection could displace the garter springs from their design locations.

The study was carried out using CDEPTH Version 5, which was the most up to date version of the code at the time. CDEPTH V5 has the capability of unloading the fuel channel down to zero load at specified fluences. However, approximations had to be made because this version of the code cannot "reload" the channel with the weight of the pressure tube, calandria tube and inspection head, and the moderator buoyancy.

The results indicate that three of the four spacers in PNGS-B and BNGS-B fuel channels will remain pinched between the pressure and calandria tubes after 15000 EFPH of operation. In the worst case, however, it may take 45000 EFPH of operation for the outboard inlet spacer to remain pinched upon de-fuelling. These numbers are likely to be conservative because of the assumptions regarding the unavailable data.

4.2.2 Range of Sag in P3/P4 at Time of Scheduled LSFCR
(N. Badie and R.A. Holt)

Another short study was carried out in response to a request from CPS to predict the range of sag in P3/P4 fuel channels at the time of scheduled LSFCR for each reactor (118,000 EFPH for P3 and 128,000 EFPH for P4). This information was needed to enable LSFCR tooling designers to allow for the maximum possible sag of the pressure and calandria tubes in their designs.

This was the first attempt to determine the range of sag in a reactor based on predictions. The study was again approximate because of the very limited number of gaugings available for comparison, and also because there has not been a gauging of more than one channel in P3/P4 since the 1979 PIP gauging of P3.

CDEPTH/CRNL-4000 predictions for seven P3 channels and one P4 channel (all central core channels) were used to obtain the average predicted sag at the corresponding fluences (118,000 EFPH for P3 and 128,000 EFPH for P4). The variation in sag due to the following parameters was also estimated: garter spring locations, outlet orientation, pressure tube creep rate, calandria tube creep rate, shape of fast flux profile and average flux. This data was then used to estimate tolerances for pressure tube and calandria tube sag in the two reactors. For instance, at 128,000 EFPH, 95% of central core pressure tubes were estimated to have deflections in the 30.0 mm to 50.1 mm range once the fuel was removed.

4.2.3 Assessment of Mock-Up Fuel Channels in SLAR Test Rig
(N. Badie and R.A. Holt)

Because of the much lower creep stiffness of the PT compared with the CT during service, the PT gradually becomes unloaded onto the CT. This corresponds to an effective interference between the free profiles of the two tubes. Concerns were expressed by SLAR tooling designers and testers that the interference between the pre-bent pressure and calandria tubes in the test rig at AECL's Sheridan Park Laboratory was more severe than in the reactors, and could cause a satisfactory SLAR system to fail the commissioning tests. The objective of this study was to determine whether the fuel channels in the test rig adequately represent the PT/CT interference in operating reactor fuel channels.

First, the accuracy of CDEPTH predictions of the interference between the PT and CT was tested by comparing CDEPTH results with in-reactor measurements for channels P3-J09 and B2-P12. Another CDEPTH run was then submitted to simulate the condition of a "worst case" Bruce 2 channel after 100,000 EFPH of operation.

The maximum deflections of PT's and CT's, and the interference between the tubes, were within the margin of the "worst case" calculation for three of the four test rig channels. The analysis also raised the possibility that the interference may be less severe than in operating reactors. We recommended

that the SLAR testing team measure the actual CT deflection in order to deduce the interference, and suggested that static upward or downward loads could be applied to the CT in order to increase or decrease the interference.

4.2.4 Other Reactor Maintenance Support
(N. Badie and R.A. Holt)

Other brief studies were also undertaken in support of the fuel channel inspection and maintenance program. These include:

- provision of contact and sag predictions for various PNGS-A and BNGS-A fuel channels which were inspected and/or gauged, using the latest version of CDEPTH and the most up to date design equations.

- calculation of the history of axial stress in BNGS-A fuel channels under different conditions (e.g. with different channel spacer locations, before and after a SLAR operation, etc.) for the purpose of circumferential flaw evaluation.

4.2.5 Contact Predictions for Point LePreau Fuel Channels
(N. Badie and R.A. Holt)

This work was initiated in response to a request from Point LePreau Nuclear Generating Station (PLNGS) for predictions of contact in 14 PLNGS fuel channels, to support the inspection shutdown of March 1989. All the channels had previously been inspected for spacer locations, and nine of them had been inspected for PT/CT contact, and gauged for sag deflection. A total of 17 functionally distinct spacers had been detected in the annulus straight region of the 14 channels (where there should be a total of 56 spacers).

The predictions were obtained with CDEPTH Version 6, and the CRNL-4000 and CRNL-4001 design equations for the PT and CT respectively. As expected (given the spacer location data), the PT's in all 14 channels were predicted to be in contact with their CT's, some over long sections of the channel (approx. 2.7 m). However, CIGAR inspection results showed either no contact or short contacts in these channels. It therefore seems that either the spacer locations or the contact indications in Pt. Lepreau are highly unreliable.

4.3 In-Reactor Deformation Mechanisms

4.3.1 Dido Program
(R.A. Holt)

Measurements have been completed for specimens with fluences up to 8.7×10^{25} n/m^2, E>1MeV. From the results to date, and from other published data (V. Fidleris, J. Nucl. Mat. 159 (1988) 22 and R.A. Holt and R.G. Fleck, COG Report CANDEV 88-142) it appears that the long-term growth rates decrease with temperature for both standard and modified (Task Group 3 - Route 1) pressure tube materials for fluences up to about 5×10^{25} n/m^2, E>1MeV. This contrasts sharply with the behaviour of cold worked Zircaloy-2 published by the UKAEA,

Figure 7, and used as the basis for the pressure tube design equation CRNL-4000. The anisotropy of the growth is observed to change with temperature, while in CRNL 4000, it is temperature independent. Hence modification of the design equation is required to more accurately reflect the temperature dependence of growth.

Preliminary theoretical calculations using a model described earlier (R.A. Holt, J. Nucl. Mat. 159 (1988) 310) predict qualitatively the correct temperature dependence, Table 5, and hence may be a suitable basis for modification of the design equations.

The absolute growth rate observed in Dido for standard pressure tube material, ie 3.5×10^{-29} m^2/n, E>1MeV, is about a factor of four lower than the elongation rate of pressure tubes. Pressure tube elongation was previously believed to consist primarily of growth and several explanations have been proposed for this discrepancy, ie:

- the growth rate in Dido is not directly relevant to the power reactor case, ie, the microstructure evolved in the power reactor environment (with stress) is different from that evolved in Dido, and hence the growth rate is different.

- the fast flux quoted for Dido is inconsistent with that quoted in the power reactors in terms of irradiation growth.

- the current measure of fast flux, ie, $n/m^2/s$, E>1MeV, is inappropriate for comparing growth results from Dido with power reactor data.

- creep constitutes a much greater proportion of the elongation rate than previously believed.

Preliminary results of experiments carried out in the past year suggest that we can reject the first explanation.

Growth specimens were machined from locations in the P4 K10 and B2 P12 pressure tubes which had accumulated 7.5 and 7.0×10^{25} n/m^2, E>1MeV, at approximately 553 and 548 K respectively. They have been further irradiated in Dido at 553 K. The results, Figure 8, indicate growth behaviour consistent with that observed in specimens of standard pressure tube material irradiated in Dido from zero fluence. This tends to rule out the second explanation given for the discrepancy between the Dido growth rates and pressure tube elongation rates.

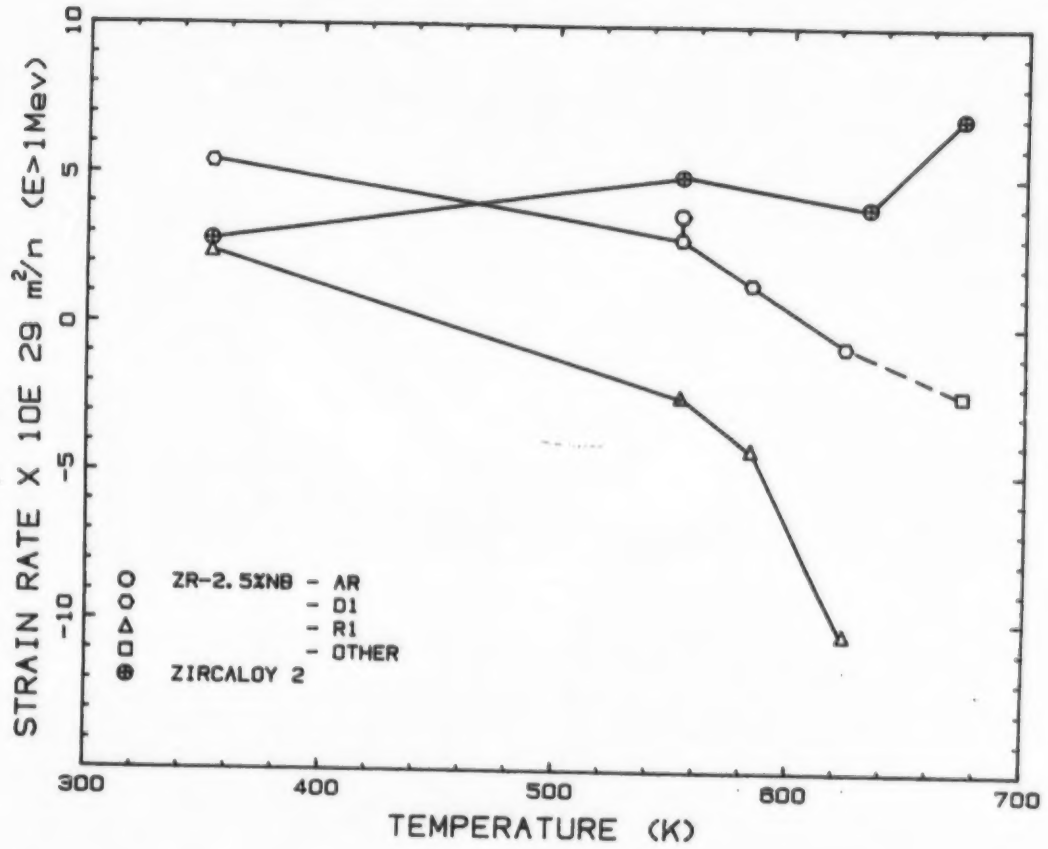

Figure 7 Temperature of dependence of the longitudinal growth of Zr-2.5% Nb pressure tube material compared with Zircaloy-2.

TABLE 5

Calculated and Measured Effects of Temperature on Longitudinal Growth Rates of Zirconium Alloys (in units of 10^{-29} M^2/N, E>1MeV)

Temperature	353/333 K	553 K	583 K
Cold-worked Zircaloy-2	3.0/3.0*	5.0/5.0*	
Std. Pressure Tube	5.7/5.4**	4.8/3.0**	4.6/0.8**
R3 Pressure Tube	3.0/2.4**	-2.1/-2.1*	-2.8/-4.3**

* Fitted/measured
**Calculated/measured

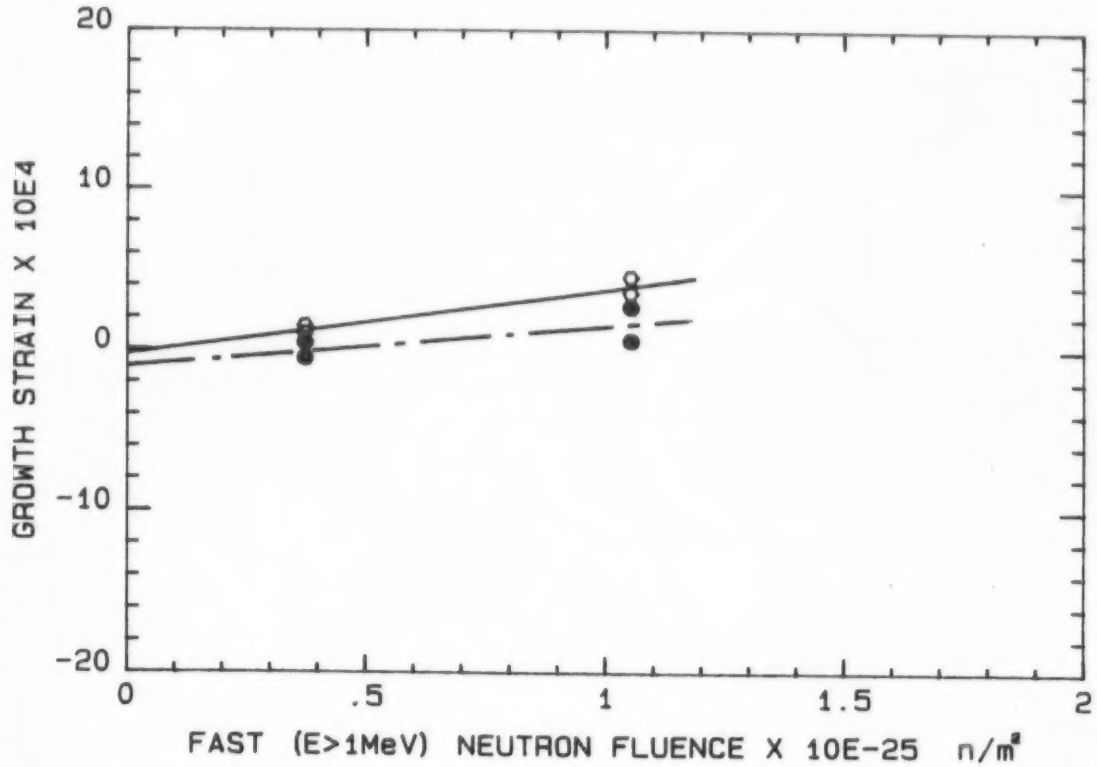

Figure 8 Growth of specimens taken from surveillance pressure tubes P4 K10 and B2 P12 (filled symbols) after 7.5 and 7.0 x 10^{25} n/m^2, E>1MeV, and irradiated in Dido.

4.3.2 **Characterization of Irradiated Pressure Tube Material**
(V. Perovic)

The preliminary TEM characterization of the irradiated microstructures of the pressure tubes of P3-J09, P4-K10 and B2-P12 and a TG3 Route 1 growth specimen from Dido were performed.

The microstructures of the pressure tubes is summarized as follows:

i) transverse foil - very high density of the <a> type dislocations and small <a> dislocation loops of 10 - 20 nm in diameter.

ii) Axial foil - relatively large number of the <c> - component dislocations. The origin of these <c>-component dislocations is not known at present but it appears in comparison with the growth specimen (see below) that they may have been generated during irradiation. This is difficult to assess with certainty because many of <c>-component dislocations are introduced into the pressure tubes during their fabrication. Besides the <c>-component dislocations, there are arrays of very fine structural features (<10 nm) observed when the foil is excited with the (0002) reflection. The exact nature of these fine features is not known at present, but they could be <c>-component dislocation loops or small beta-Nb particles precipitated during irradiation.

iii) Radial Foil - The appearance of the second phase clearly indicates considerable transformation towards the beta-Nb phase during operation.

The microstructure of the growth specimen is characterized as follows.

i) transverse foil - as in the surveillance tubes, a very high density of (a) type defects. The previous dislocation networks composed of <a>-dislocations (<a>/<a> sub-boundaries) have started to disintegrate. Arrays of <a> type defects were also observed, resembling rows of dislocation loops which may result from an autocatalytic nucleation process or punching out from an area of high stress concentration.

ii) Axial foil - a relatively high density of the <c>-component defects, Figure 9. As previously reported one of the major characteristic of the Route 1 material is that the alpha-grains are mostly free of <c>-component dislocations, Figure 9A. Hence the <c> component dislocations in Figure 9B clearly result from irradiation. They are always tightly connected to the alpha/beta interface suggesting that they might be associated with the transformation of the β-phase or with the internal stresses created during irradiation.

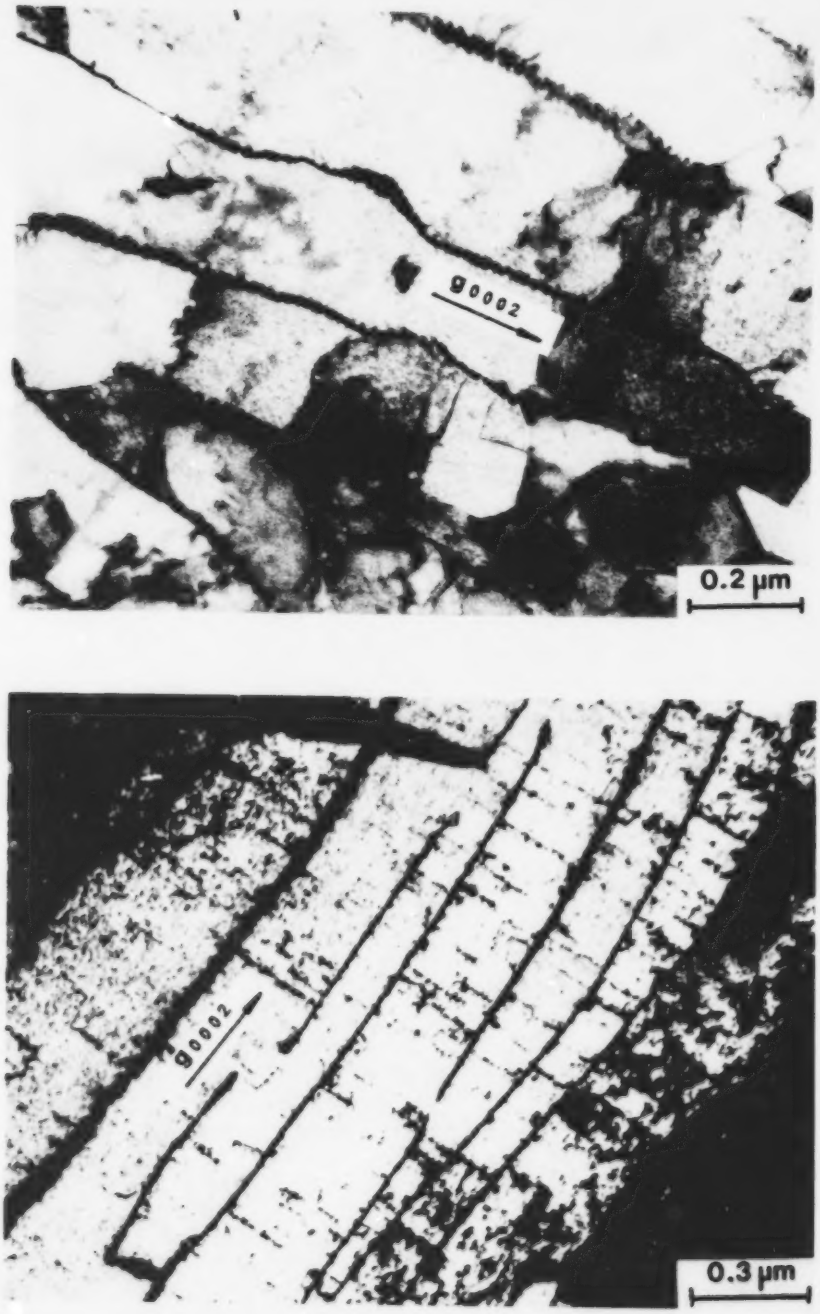

Figure 9(a-b) Microstructure of TG3 route 1 pressure tube material: A - before irradiation, showing grains free of <c>-component dislocations, and B - showing <c>-component dislocations formed during irradiation to 2×10^{25} n/m^2, E>1MeV.

4.3.3 Osiris Program
(R.A. Holt)

A contract was signed with the CEA (France) in June 1988 to irradiate 42 growth specimens and 7 pressurized creep capsules to end-of-life fast neutron fluences in the Osiris reactor at Saclay (fast flux = 2.2×10^{18} $n/m^2/s$, E>1MeV). The preparation and characterization of specimens and the measurement of the growth specimens is being carried out by AECL. The specimens were delivered to Saclay and preirradiation qualification of the growth measuring rig in a hot cell was carried out 1988/11.

The measurement of the creep capsules will be performed by the CEA using underwater apparatus designed for and dedicated to the program. Preirradiation measurements were carried out 1989/03 at Saclay and on 42 diameter measurements agreed to within 1 μm with measurements made at CRNL prior to delivery of the specimens.

The fast flux for the experiment and for end-of-life fracture properties experiments is being assessed by irradiating flux and displacement damage monitors in Isis, the low power mockup of Osiris. The first run of Isis was completed 1989/03. The resultant measured vertical fast flux profile is shown in Figure 10 relative to the specimen positions for the three experiments. The maximum flux gradient, about 13%, will occur in the uppermost creep capsule. The flux gradient in the uppermost growth specimen will be about 10%.

The preparation of the insert for the irradiation is complete and is scheduled for insertion for irradiation in the Osiris cycle starting 1989/04/25. This is a delay of five months relative to the schedule proposed to COG 1987/12 due to the unexpected complexity of the insert design. The first measurement campaign will be carried out after 3 cycles in Osiris 1989/09.

4.3.4 Evaluation of Power Reactor Fast Fluxes
(R.A. Holt)

To evaluate the CANDU fast flux spectrum close to the pressure tube and to assess the effect of this environment on the deformation and fracture properties of pressure tube materials.

Fabrication and preparation of the first three bundles is complete and they have been delivered to the station. The station proposal for the program received formal AECB approval in 1989/01 and the three bundles have been scheduled for loading into Bruce Unit 4 in the period 1989/04 - 1989/05.

A contract let to AECL Candu Operations to oversee the design of tooling and the writing of procedures for assembling carrier bundles containing preirradiated specimens is underway. Estimates of the gamma fields have been made, design concepts for the tooling and procedure have been developed and design is in progress.

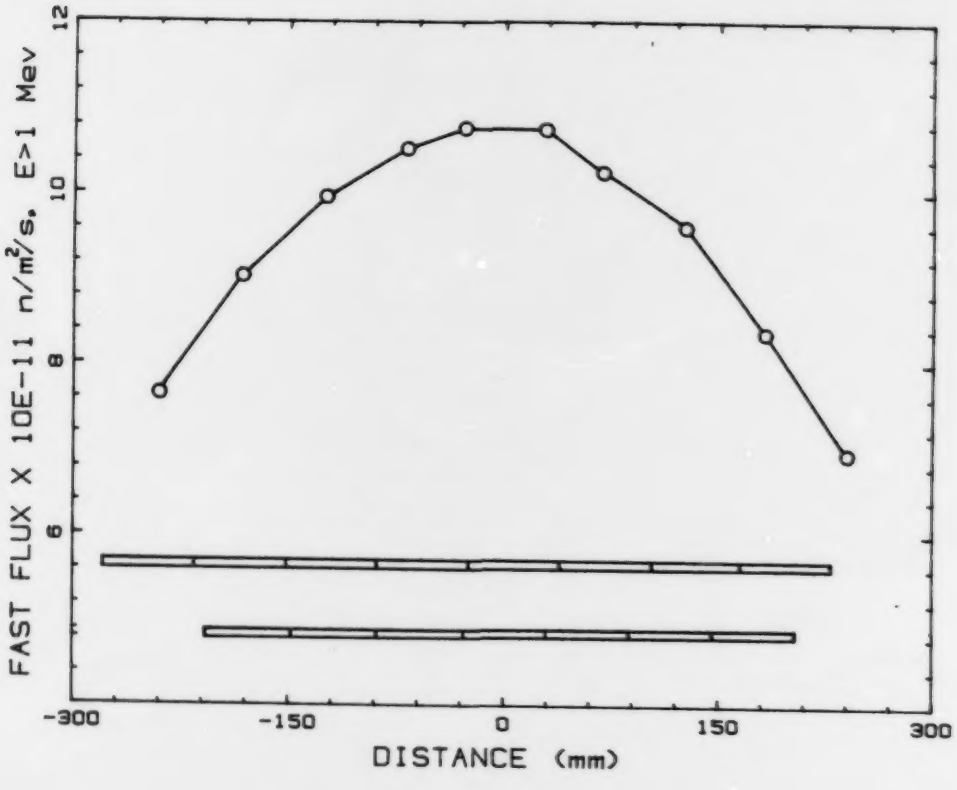

Figure 10 Flux profile relative to reactor centreline observed in a mockup of the Osiris inserts during a run of the Isis reactor. The Osiris flux is 200 times that in Isis. The bars indicate the disposition of fracture (top bar) and creep and growth (bottom bar) in the reactor core.

4.4 The β to α Transformation in a Zr-2.5 WT% Nb Alloy
(V. Perovic and R. Jarochowicz)

The transformation has been studied by transmission electron microscopy. The complex arrays of dislocations observed at the α/β interface were associated with <a+c> slip on $(\bar{1}101)_H$ planes and interactions of <a> dislocations with the <a+c> arrays. The <a+c> dislocations lay parallel to the intersection of $(\bar{1}101)_H$, $(110)_B$ with the cone of unextended lines of the transformation. The interaction between <a> and <a+c> dislocations at the interface were analyzed by considering the similarities between step formation at tilt boundaries in single phase alloys and those found at the α/β interface in the present alloy. The work was done in collaboration with Prof. G.C. Weatherly (University of Toronto) and performed was published in Acta Metallurgica.

4.5 C-Component Dislocations in Sub-Boundaries in a ZR-2.5 Wt% Nb Alloy
(V. Perovic)

A typical processing schedule for Zr-2.5 wt% Nb alloys is extrusion in a temperature range which straddles the α–β phase field. After extrusion, the microstructure of the alloy consists of an elongated array of retained β_{Zr}-plates linked by sub-boundaries in the α–phase. The majority of the sub-boundaries contain <c>-component dislocations. These arrays of sub-boundaries are stable on annealing below the β-transus. In this work, the geometry of the sub-boundaries composed of <c>-component dislocations is analyzed. It was shown that the <c>-component dislocations are contained in both, tilt boundaries and twist boundaries;

4.5.1 Tilt Boundaries

When the pure tilt boundary formed by <a> dislocations is rotated the <c> dislocations are incorporated in the structure. The rotation of the boundary is localized to the <c> dislocations, ie, a step structure is formed. As the number of <c> dislocations increases, the rotation of the macroscopic boundary plane increases forming on asymmetrical boundary. The diffraction contrast from the <c> dislocations showed double images separated by about 3-4 nm at many steps. The contrast is thought to arise from the dissociation of <c> or <c+a> dislocations.

4.5.2 Twist Boundaries

A general grain boundary can be described by three sets of dislocations having independent Burgers vectors. We have found in general than in Zr-Nb alloy this class of boundary can be broken down into two types. In the first, one set of <a> dislocations and the <c> dislocations cross each other nearly orthogonal with little interaction. The second set of <a> dislocations crosses at an oblique angle. This set interacts with both the first set of <a> and <c> dislocations. At each junction point, a complex series of nodes has to be established so that the net Burgers vector at each node sums to zero.

In the second type of boundary both sets of <a> dislocations cross the <c> dislocations at an oblique angle. Again, a complex series of reactions and nodes must be developed at the point where 2<a> and <c> dislocations meet. We believe that the majority of the <c>-component dislocations are introduced during high temperature deformation processing of the alloy. There are two sources of <c>-component dislocations - pyramidal slip and the $\alpha=\beta$ phase transformation.

Particular emphasis is placed on the role of <c>-component dislocations in the sub-structure. As climb of dislocation with a <c> component will lead to strain in this direction, there has been some interest in the role played by these dislocations during in-service irradiation. The work is in a written stage which we intend to submit for an external publication. This study is performed in collaboration with Prof. G.C. Weatherly.

4.6 **Pressure Tube Development**
(R.A. Holt, R.G. Fleck,
M. McGraw, P. Vesely,
A. Donner, R. Jarochowicz
and A. McMillan)

The first batch of pressure tubes (1988-1) made for NSD to the Task Group 3 Route 1 (TG3 R1) specification in 1988 exhibited rejectable ultrasonic indications on the ID. These were found in 75% of the tubes after honing following the final draw. Metallurgical sectioning revealed a good correlation in size and location between the ultrasonic indications and shear (45°) cracking.

A review of the fabrication procedures revealed that the only difference to which any significance could be attributed compared with the pilot order of tubes made in 1980 was a reduction in the number of drawing passes from four to three. Hardness traces through the wall of a tube exhibiting cracks showed no gradient which might indicate segregation or strain gradients.

A batch of 13 more tubes (1988-2) were made from another ingot with the four draw schedule. These exhibited a 56% rate of cracking. Inspection between draws showed that the cracks appeared during the final draw. The tubes were honed for inspection between draws and hence the total cold-reduction was less for 1988-2 than for 1988-1 or 1980 batches (38% vs 40% vs 42%). Tensile tests revealed that 3rd draw material exhibited ductility (see below) and no significant difference was found in strain rate sensitivity between TG3 3rd draw material and standard pressure tube material with a similar level of cold-work. SIMS and Auger spectroscopy revealed no segregation or contamination of the ID surface.

Rolling trials were undertaken comparing strips cut directly from an extrusion of one of the 1988-2 pressure tubes and a standard pressure tube. Cracking was found in the TG3 material after 40% cold-work, whereas none was observed in the standard material. This appeared to be related to the surface finish.

When the rolling trials were carried out on flat bars milled from the extrusion both standard and TG3 materials were rolled 59% with no cracking. Hence the problem does not appear to be one of low bulk ductility.

The tubes of the 1988-01 and 1988-02 batches were found to contain more oxygen than those of the 1980 pilot order, Table 6. The difference is not great enough to be of concern but could potentially contribute to the apparent increase in the tendency to crack during drawing.

Table 6
Results of Oxygen Analysis of TG3 Pressure Tubes

Ingot/tube	Number of Samples	Oxygen Concentration ppm	Standard Deviation ppm
1980	10	1379	39
1988 - 1	7	1471*	15
1988 - 2	7	1444*	11
TG 061 ID	3	1467	6
Midwall	3	1483	21
OD	3	1493	6
Tg 061 All	10	1481	15

* Significantly different from 1980 ingot at 95% confidence level.

Consultation was arranged with Prof. B. Avitzur of Lehigh University by CANDU Operations. His recommendation was that the incidence of cracking might be reduced by reducing the semi-cone angle of the drawing die from the current 15°. A purchase order is being placed with Nutech to produce three tubes from existing 1988-2 extrusions.

Pilgering was suggested as an alternate route for cold working the tubes because up to 80% cold-work has previously been introduced into Zr-2.5% Nb fuel cladding by this technique without problems. An order was placed through Nutech Precision Metals for the pilgering of five extrusions from the same ingot as the 1988-2 batch by Haines International in Arcadia, Louisiana. The first tube pilgered had circumferential ID cracks, visible at low magnification, which were clearly related to circumferential marks left by the honing and polishing operations. Subsequent examination revealed these not to be shear cracks but to have a "V" shaped profile. The deepest one examined was 0.07 mm deep. This, and the experience with rolling suggest that the cracking may be associated with surface condition in the case of pilgering. The next tube was pickled to remove 0.15 mm from the ID surface before pilgering and we are awaiting results of the UT inspection of this tube.

4.7 Tensile Evaluation of TG3 R1 Tubes

(G.K. Shek and H. Seahra)

A high percentage of production TG3 Route 1 tubes developed shear cracks at the inside surface during the fourth and final cold draw pass. Test materials were obtained after each cold work stage in order to determine the change in tensile properties as a function of cold work. Two TG3 extrusions from the development program which produced tubes free of cracks were also included in the test program for comparison. The test results showed that the current batch of extrusions had similar tensile properties to the development extrusions. Tensile strength increased with cold work up to the third draw. For a given level of cold work, there was a significant amount of scatter on the results of yield strength and ductility. The scatter was probably due to the fact that specimens at a given level of cold work were machined from different tubes. However, the tubes still had good ductility after the third draw. The tensile properties of the samples after the fourth draw was unexpected in that it displayed a lower yield strength and improved ductility compared to that after the third draw. Subsequent investigation indicated that the tubes from which the fourth draw samples were taken had been stress relieved at 500°C.

4.8 Tensile Properties of Zr-2.5 Wt% Nb Pressure Tube Materials Under High Applied Strain Rate Conditions

(E.T.C. Ho and M. McGraw))

A test program has been initiated to investigate the tensile properties of Zr-2.5 Wt% Nb pressure tube (PT) material under high applied strain rate conditions over the temperature range room temperature to 100°C. This work was precipitated by the observation of shear cracks in some of the 1988 batch of TG3 Route 1 pressure tubes, which appeared after the third cold draw. Analysis of die dimensions and other processing parameters indicates that the local strain rate during cold reduction was in the order of 3×10^{-1} s^{-1} and that heating of the tube due to cold working was in the order of 25°C. Based on the results of such an analysis, a matrix of test conditions was established. These test conditions include applied strain rates of 3×10^{-2}, 3×10^{-1} and 3 s^{-1} and temperatures of ambient temperature, 50°C and 100°C. Pressure tube materials examined to date include as-cold-worked Darlington-type (H1587) and three pass cold draw TG3 Route 1 (TG082) axial tensile specimens.

Results obtained to date indicate that both types of Zr-2.5 Nb PT materials were strain rate sensitive over the range of strain rates and temperatures investigated. However, the difference in strain rate sensitivity between the Darlington-type and the three draw TG3 materials was marginal, as shown in Figures 11 and 12. The high strain rate data also showed that the three draw TG3 material was significantly stronger than the Darlington-type material. Some four pass cold draw TG3 materials have been obtained from Nu-Tech. These materials will be tested under high applied strain rate conditions as well.

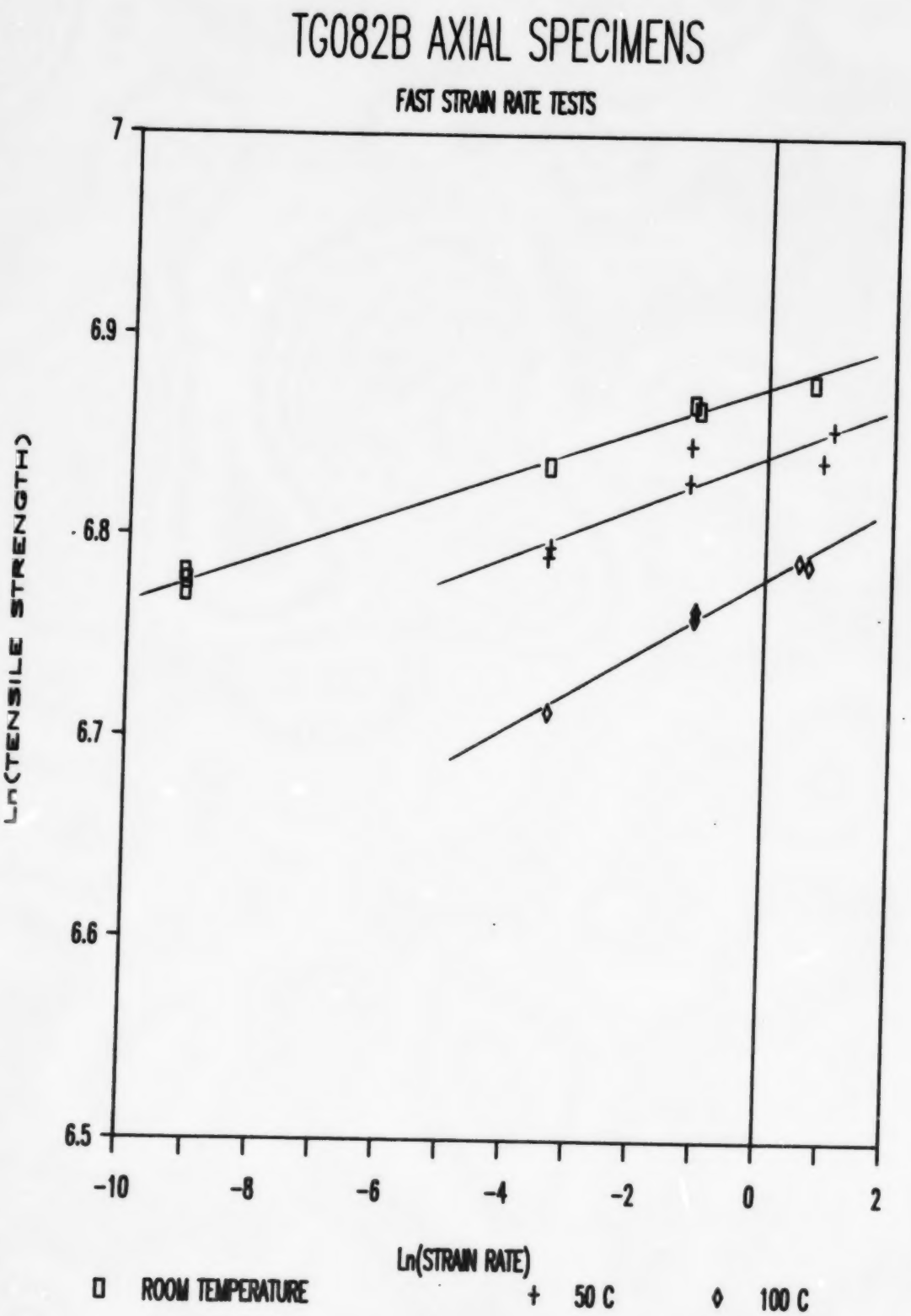

Figure 11: Plots illustrating variation of longitudinal tensile strength with applied strain rate in three cold draw TG3 Route 1 Zr-2.5 Nb pressure tube material.

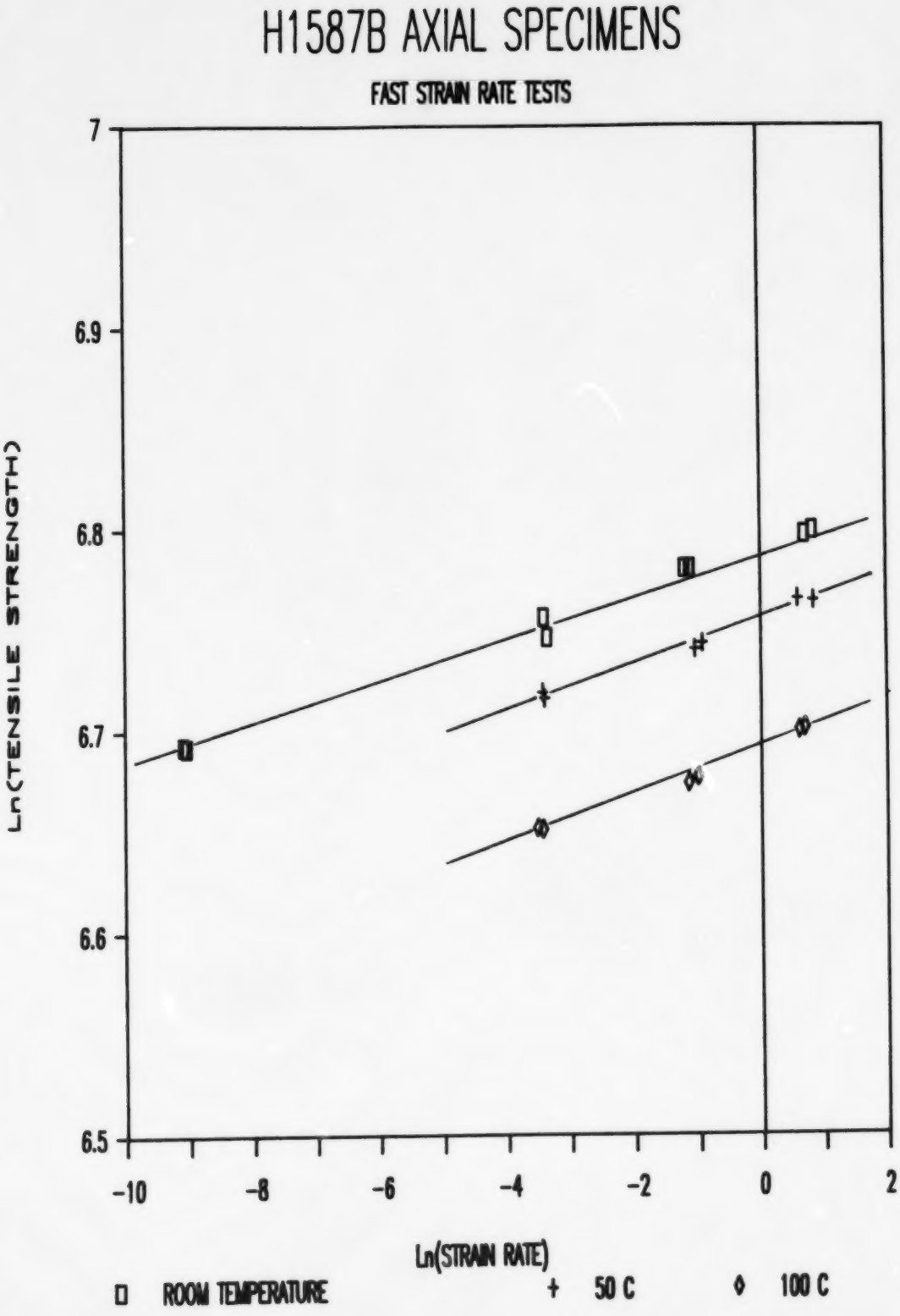

Figure 12: Plots illustrating variation of longitudinal tensile strength with applied strain rate in as-cold-worked Darlington-type Zr-2.5 Nb pressure tube material.

Based on the information obtained to date, it does not appear that the rate sensitivity of the Zr-2.5 Nb PT material plays an important role in the occurrence of shear cracks in the 1988 batch of TG3 Route 1 pressure tubes. However, the relatively high flow stresses and low limits of uniform strain (typically 2-3%) of the as-cold-worked three draw TG3 material may make it susceptible to shear cracking during subsequent cold drawing.

4.9 Steam Oxidation, Biaxial Deformation and Beryllium-Assisted Crack Penetration Behaviour of CANDU Reactor Zircaloy-4 Fuel Cladding at Elevated Temperatures

(E.T.C. Ho/A. Donner)

4.9.1 Steam Oxidation Kinetics

This test program produces oxidation kinetic data suitable for use in the analysis of the oxidation behaviour of both as-received parent and braze HAZ Zr-4 fuel cladding materials in a steam environment for temperatures in the range 600-850°C.

In a given test, empty Zr-4 fuel cladding specimens (complete with bearing and spacer pads) back-filled with argon gas were exposed to a flowing steam environment in a stainless steel reaction chamber inside a tube resistance furnace. The temperatures and times at temperature investigated were similar to those used for the air oxidation experiments carried out previously. Immediately following the high temperature exposure, the Zr-4 specimens were quenched in a water bath of tap water at about 10°C.

Analysis of the steam oxidation data indicates that the rates of oxidation of both parent and braze HAZ materials in steam were lower than those observed in air, with the possible exception of parent material at 650°C. At this temperature, the parent material oxidizes at very similar rates in the two environments. A summary of the steam oxidation data is presented graphically in Figures 13-14. The oxidation behaviour of parent material appears to obey linear oxidation kinetics in steam for temperatures up to about 750°C. Above this temperature, the oxidation rates fall dramatically and the rates appear to obey parabolic rate kinetics, at least over the range of times examined experimentally. In contrast, the braze HAZ material appears to obey linear kinetics over the entire range of temperatures investigated. However, the rate at 850°C was lower than those observed at 750 and 800°C.

Data obtained from preliminary analysis of the microstructure of the underlying metal substrate indicate that it was gradually transforming to B-Zr phase due to the absorption of hydrogen produced by the Zr-steam oxidation reaction. The observed differences in oxidation rates in air and in steam may be related to this phenomenon.

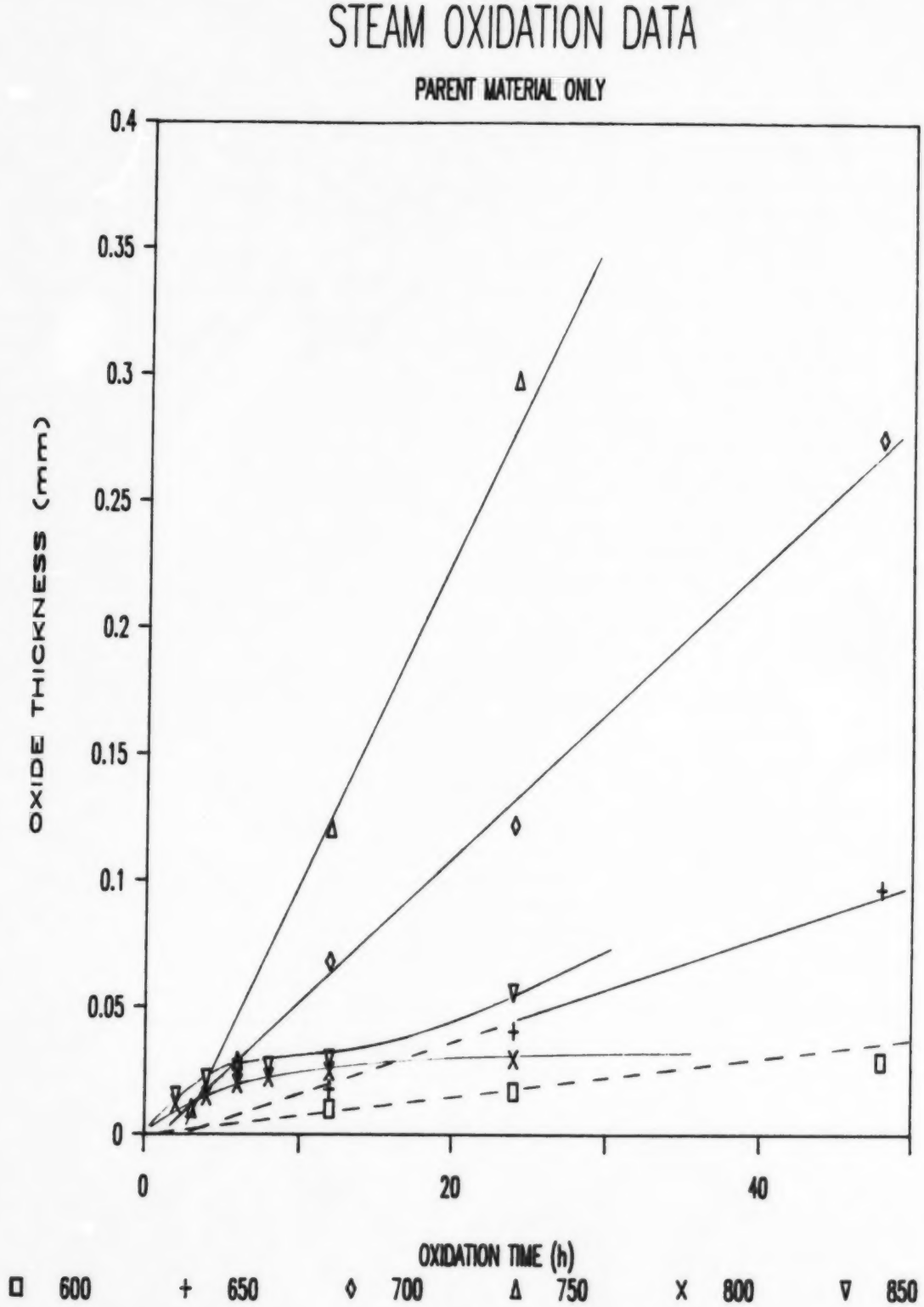

Figure 13: Oxidation data for parent Zircaloy-4 fuel cladding in a steam environment.

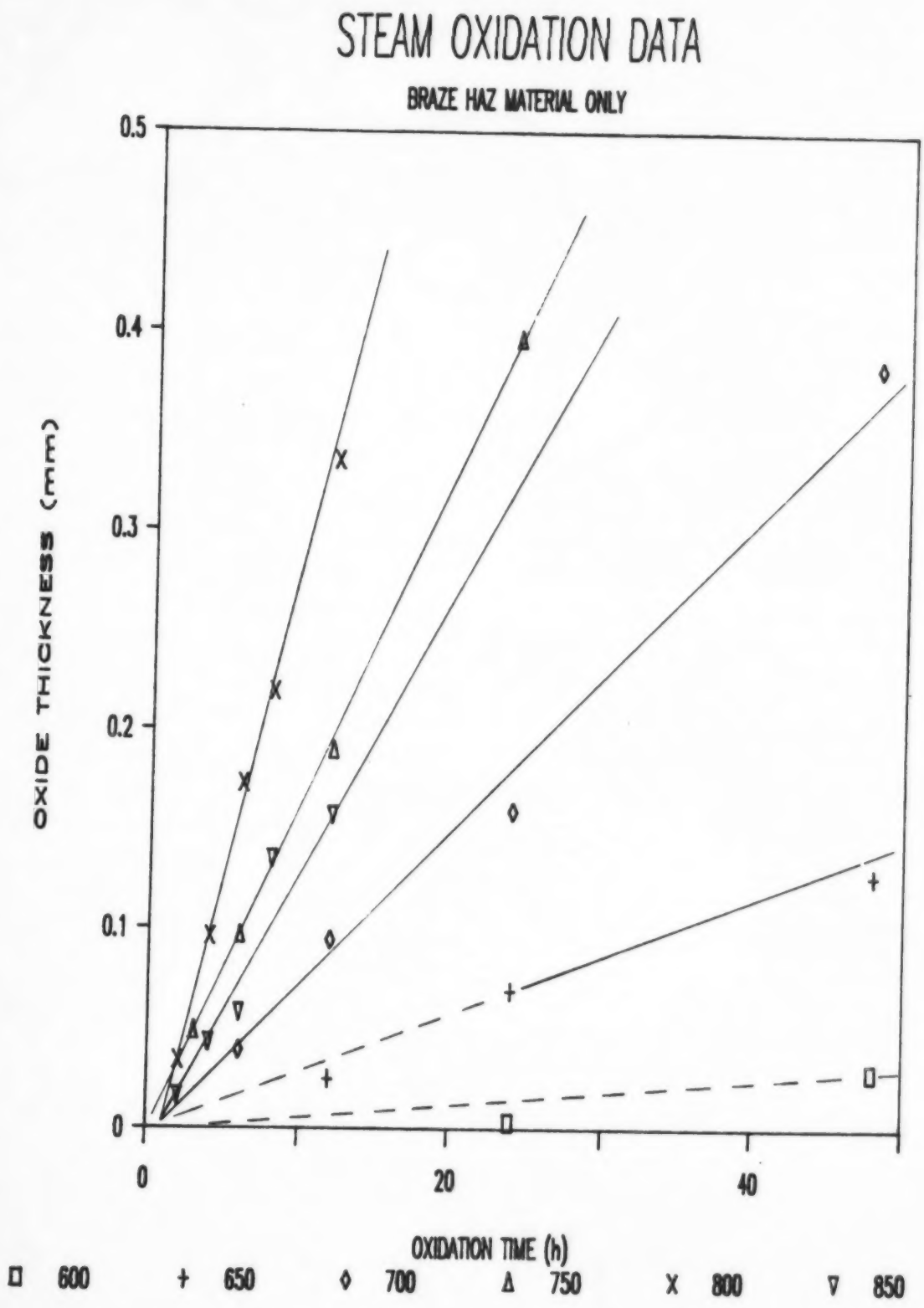

Figure 14: Oxidation data for braze heat-affected-zone (HAZ) Zircaloy-4 fuel cladding in steam.

4.9.2 Biaxial Deformation Behaviour in Air

This test program produces data suitable for use in the analysis of the biaxial deformation behaviour of Zr-4 fuel cladding material under postulated degraded cooling conditions and fuel handling incidents.

In a given test, empty Zr-4 fuel cladding samples were evacuated and pressurized with argon and exposed to test temperatures in the range 400-850°C at 50°C intervals. At each temperature and pressure, the samples were allowed to go to failure or to a maximum exposure time of 14 days. The time from initial ramp to failure was recorded using a one second resolution counter.

Analysis of the ruptured specimens indicates that failure of the pressurized cladding samples resulted from several competing processes which include:

a) loss of wall thickness due to oxidation of the metal substrate;

b) loss of wall thickness due to straining or ballooning of the weaker parent material;

c) beryllium braze penetration and/or interactions between the bearing and spacer pads and the underlying braze HAZ cladding metal.

At a given temperature, the mode of failure is determined principally by the strength of the parent material relative to the applied internal differential pressure which is maintained constant via an expansion tank. For a sufficiently large differential pressure, the failure is dominated by ballooning of the parent material. However, at low pressures, the failure is dominated by rupture in the bearing/spacer pad-cladding interfacial regions in the braze HAZ. At intermediate pressures, where the wall reduction mechanisms described above have similar impact, the failure can either be in parent or in braze HAZ materials. Data presented in Figure 15 illustrate the above observations clearly.

4.9.3 Beryllium-Assisted Crack Penetration Behaviour at Elevated Temperatures

This test program is designed to produce data which extend the data base currently available for analysis of Be-assisted crack penetration behaviour in air, to steam environments and also to temperatures in excess of 1000°C.

To date, induction heating and auxiliary equipment capable of heating fuel cladding samples in steam to temperatures in excess of 1000°C have been acquired and built. Preliminary experiments carried out indicate that the existing induction heating system will have to be modified slightly to accommodate the new heating requirements.

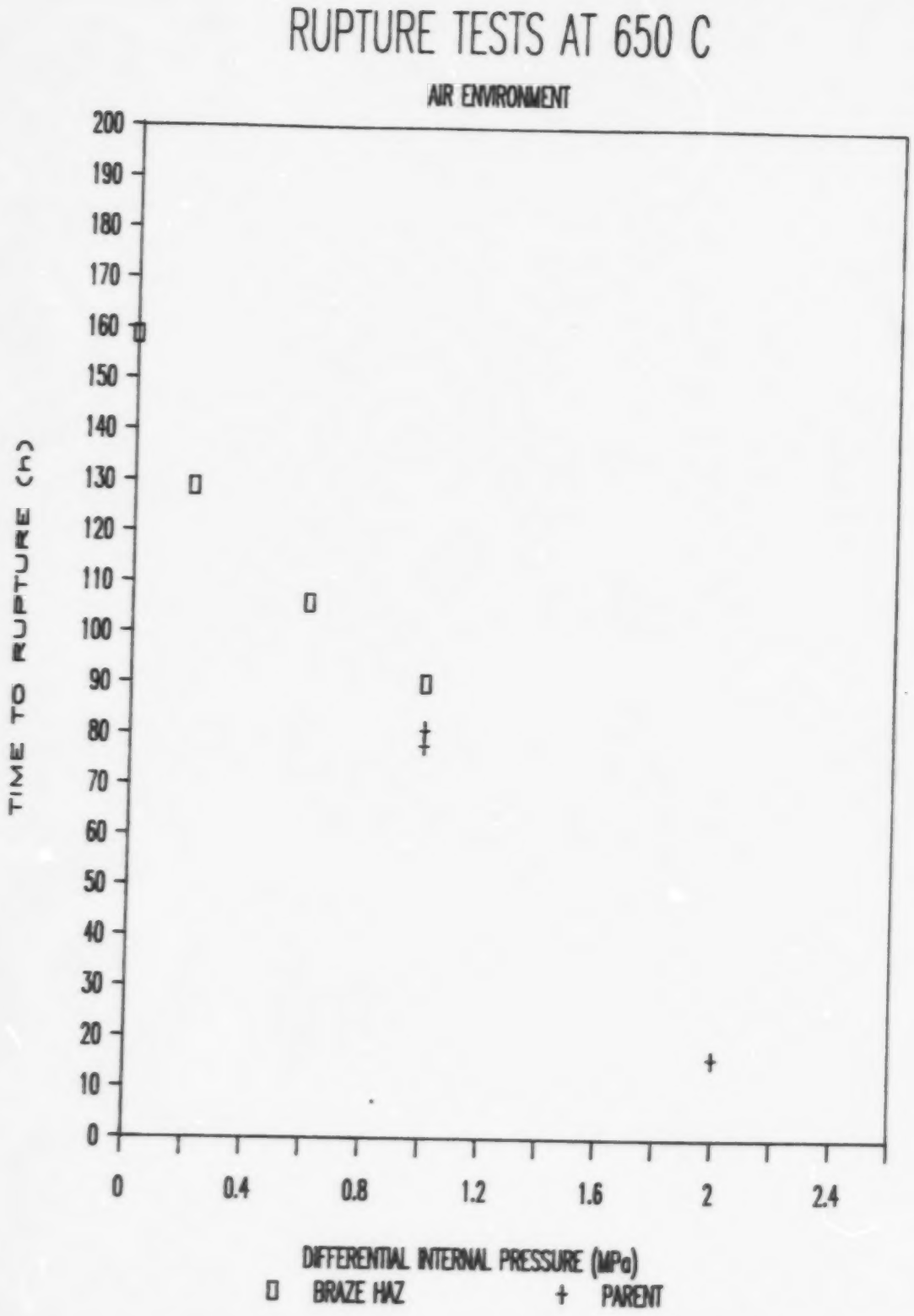

Figure 15: Plot illustrating rupture behaviour of Zircaloy-4 fuel cladding samples in an air environment. Rupture can occur in both parent and braze HAZ materials.

4.10 Miscellaneous Tensile Testing Using the Computer-controlled Materials Characterization Test Facility

Several small tensile test programs were undertaken using the servohydraulic computer-controlled Materials Characterization Test Facility (MCTF) in the past year. The more notable test programs carried out include:

1. A high priority tensile test program for J.M. Boag of the Mechanical Research Department. The material tested was Bruce NGS "A" PHT pump hold down bolt material (SA193-Gr B7).

2. Tensile testing of A356-SiC composite materials in support of the Division's Advanced Industrial Materials (AIM) research program.

3. Monotonic and cyclic tensile testing of SA210-A1 boiler tube material at ambient temperature and 274°C in support of the EPRI-funded corrosion fatigue project. (E.T.C. Ho and M. McGraw)

4.11 Tensile Properties of Darlington PHT Piping Material

(E.T.C. Ho and M.J. McGraw)

On request from Mechanical Design Department personnel (M.J. Kozluk), a test program was carried out to extend the tensile data base for Darlington PHT piping material to 22" elbow and 21" NPS pipe materials. Test programs conducted previously had generated extensive tensile data for: a) SA106B 12", 22" and 24" NPS parent piping materials; b) SA105 vesselet material; c) various weld and weld heat-affected-zone (HAZ) materials. The above tensile data, together with J-resistance data generated elsewhere provide the necessary materials data needed to carry out a leak-before-break analysis for the Darlington PHT piping system.

The main results obtained from the above test program may be summarized as follows:

1. The yield strength and the tensile strength of the 22" elbow material at 250°C are about 10% and 17% lower than those of the 22" parent piping material.

2. The yield strength and the tensile strength of the 21" NPS piping material are intermediate between the respective tensile properties of the 12" and 22" NPS parent piping materials.

3. Both types of material exhibited serrated flow behaviour at low strain levels (ie, from yielding to a few % strain).

4. The yield strength and tensile strength of both materials showed no measurable directional dependence. Only the % reduction of area was detectably lower in the circumferential direction.

5. Based on the observation of serrated flow, both materials are expected to be strain rate sensitive at 250°C.

4.12 Method to Initiate ID Cracks in Zr-2.5 Wt% Nb Pressure Tube Samples

(E.T.C. Ho and M. McGraw)

A method to produce sharp fatigue cracks in the ID surface of a section of Zr-2.5 Nb pressure tube without the use of a machined flaw for stress concentration has been developed. This method is based on an experimental procedure developed for producing ID-initiated corrosion fatigue cracks in thermal plant boiler tube specimens for an EPRI-funded project.

A schematic diagram of the loading rig for cyclic compression of Zr-2.5 Nb PT samples is shown in Figure 16. When the tube specimen is compressed, the ID surface strains in the circumferential or hoop direction at the 0° (top) and 180° (bottom) locations are tensile in nature while the circumferential strains at the 90° and 270° locations are compressive in nature. Using the above loading rig, a tube specimen can be cyclically loaded to produce cyclic circumferential tensile strains at the 0° and 180° locations. If the peak compressive load is large enough, the induced circumferential tensile stress in the ID surface at the 180° location should be above the yield stress and a fatigue crack would be initiated after a sufficient number of cycles for a given compressive load.

Figure 17 presents an example of strain gauge data obtained from loading a 30.48 cm (12") long Zr-2.5 Nb PT specimen which had been instrumented with axial and circumferential strain gauges on the ID surface at the 0°, 90°, 180° and 270° locations. The data show clearly that the maximum loading occurs at the 180° or bottom location. To date, axial ID-initiated fatigue cracks have been produced in several Zr-2.5 Nb tube samples ranging from 15-30 centimeters in length. However, the experimental technique requires additional refinement before ID-initiated fatigue cracks of prespecified depths can be produced in a reliable and consistent manner.

4.13 Inert Atmosphere Testing of Thermal Plant Materials

(M. McGraw and R.A. Holt)

Assessment of the remaining life of thermal generating stations requires the assessment of creep damage to components in service, often by testing of specimens removed from the actual components. In the latter case the availability of material is usually limited and it is necessary to test subsize specimens. To limit the effects of oxidation on the results it is desirable to test such specimens in an inert atmosphere. In response to this requirement, Materials Integrity Section has developed the capability of testing such specimens in argon.

Figure 18 shows the results of seven tests carried out on standard and subsize specimens of SA 213 Grade T22 boiler tube material. The specimens had nominal gauge dimensions of 50 mm long x 8 mm dia. or 15.9 mm long x 2.86 mm dia.

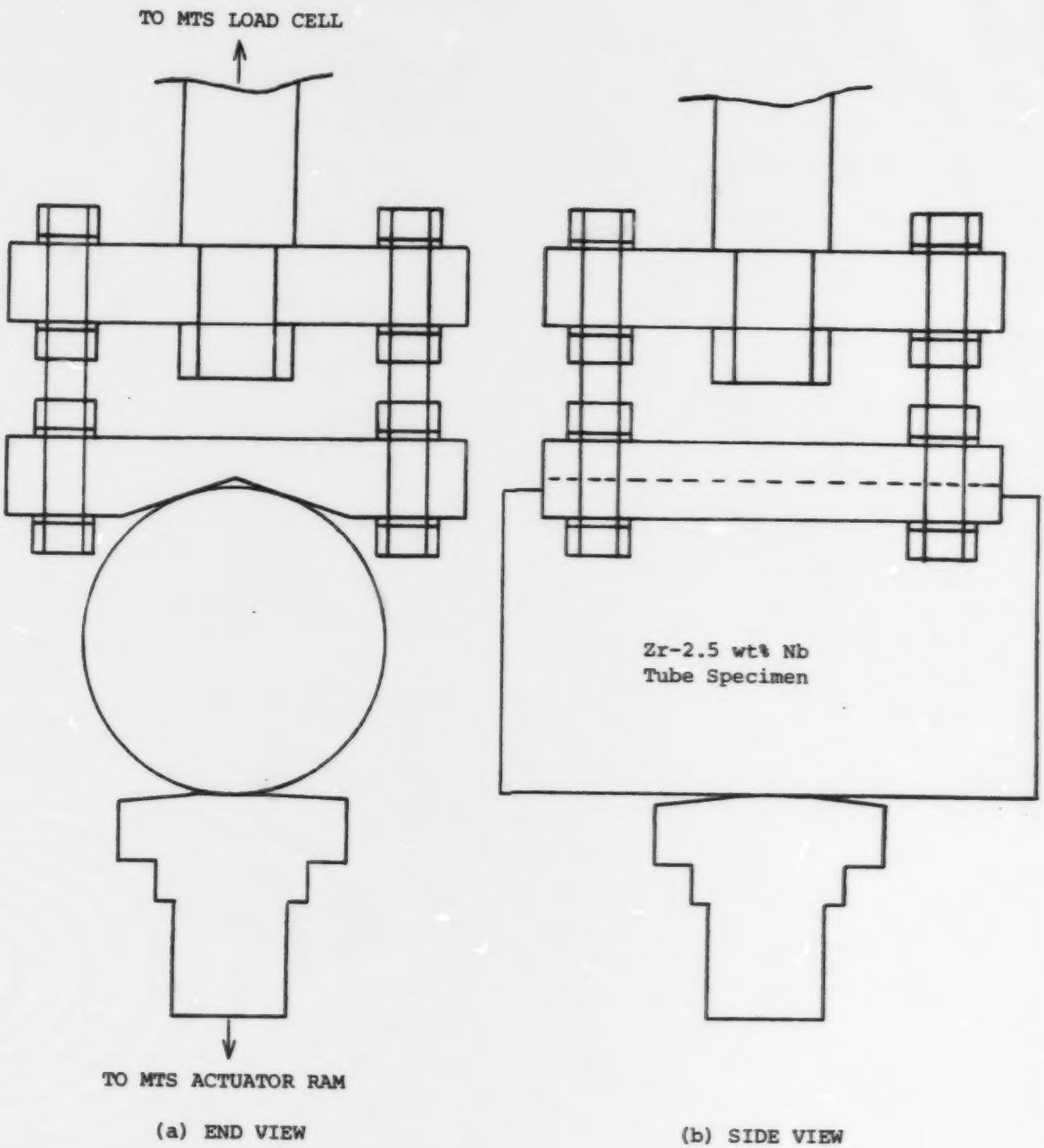

Figure 16 Schematic diagrams illustrating the basic design of the current test rig for cyclic compressive loading of Zr-2.5 wt% Nb pressure tube specimens.

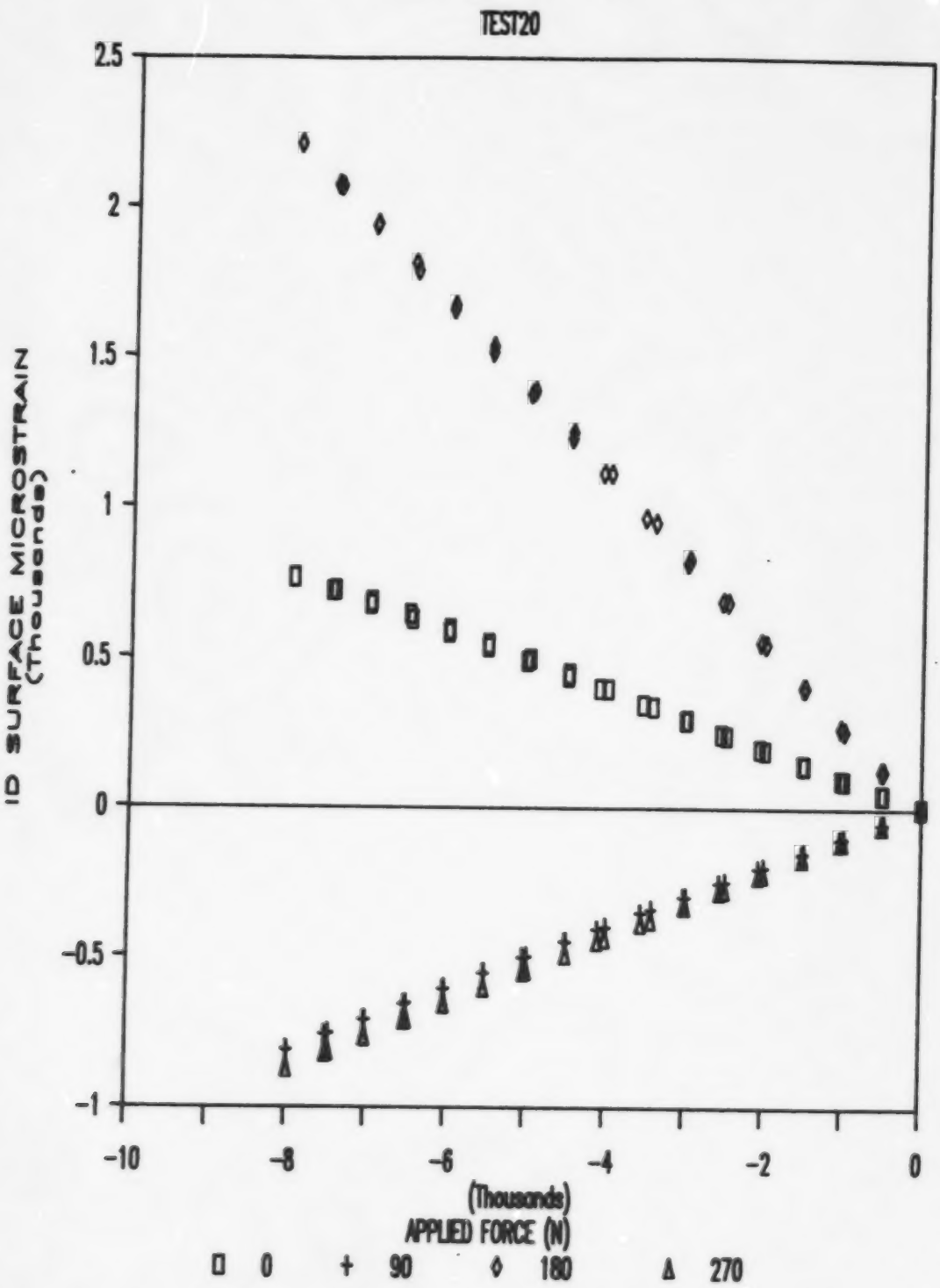

Figure 17. Strain gauge data showing the loading behaviour in a Zr-2.5 wt% Nb pressure tube specimen under compressive loading conditions.

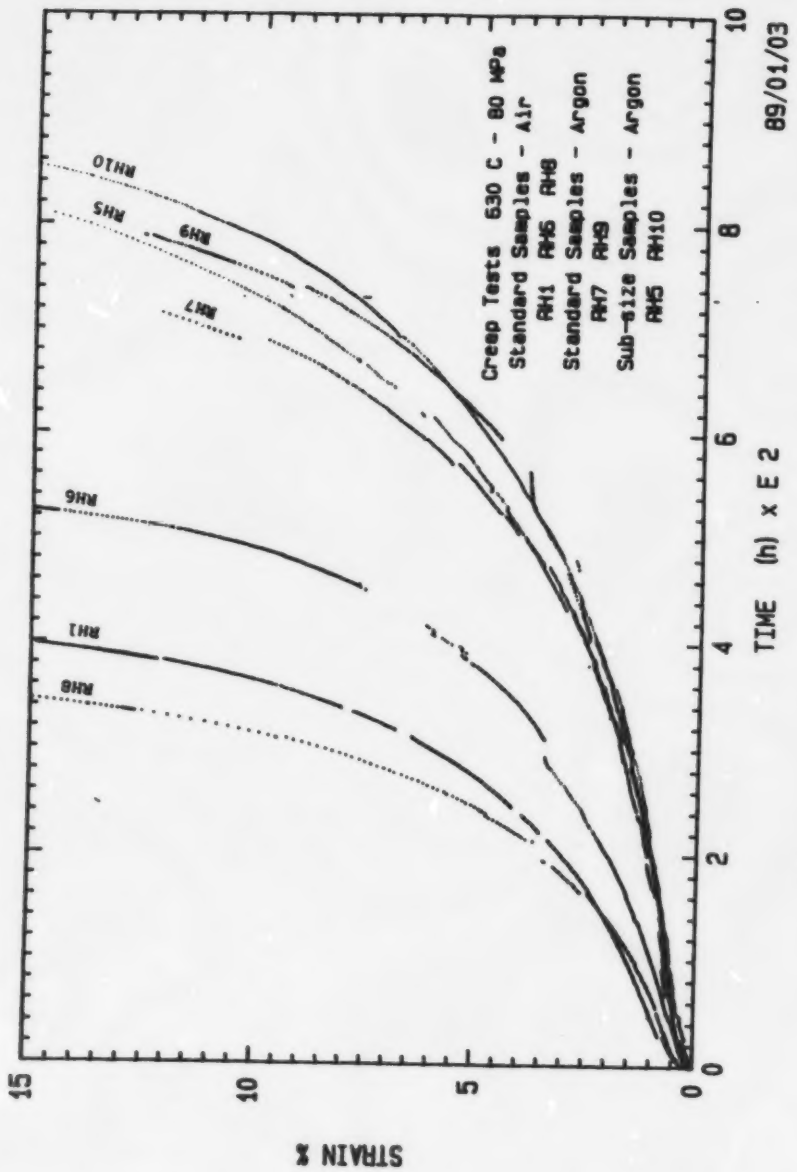

Figure 18 % Strain Verse Time for Air and Argon Tests 630C/80 MPa

respectively. All specimens were tested at 903 K at a stress of 80 MPa. The standard specimens were tested in air (tests RH1, RH6 and RH8) or in Ar (tests RH7 and RH9). Small specimens were tested only in Ar (tests RH5 and RH10).

The inert atmosphere reduced the creep rate and increased the time to fracture of the standard specimens by about a factor of two, probably because the cross-section was not reduced by oxidation during the test. The behaviour of the subsize specimens in Ar was very similar to that of the standard specimens, verifying the validity of the testing technique for the subsize specimens.

Materials Integrity Section is now in a position to respond to requests from Central Production Services to perform creep tests on samples of thermal plant components.

5.0 SEM PROGRAMS

(S. Sandloehken)

The JEOL 840A scanning electron microscope was extensively used in support of long-term projects performed by the Corrosion and Tritium Technology Section and the Corrosion Chemistry and Decontamination Section. For these Sections the main areas of study were steam generator and heat exchanger corrosion. The SEM was used for EDX analysis of the distribution of various elements, on the surface of corroded test specimens, expected to be associated with the corrosion process. Examination of both metal and deposits, such as secondary side steam generator sludge, removed from plant components were also performed. In support of programs in the Materials Integrity Section the SEM was used to examine the surfaces of TG3-R1 pressure tube material that had cracked in production. The examinations were performed to determine if local concentration of alloy or trace elements had occurred.

In total the SEM was used to support work program in fifteen Sections of the Division, with the above being the main clients. Program co-ordination was also provided for work that was contracted out to Centre for Microscopic Characterization of Materials and Surface Science - Western.

1989 PROGRAMS

6.0 FRACTURE MECHANISMS UNIT

6.1 Blisters

6.1.1 Probabilistic Modelling of Tube Fracture Due to Blisters for Reactor Assessment

Develop and use a probabilistic computer model of pressure tube fracture due to blisters for making reactor assessments.

Continue to model development to incorporate any new results from blister related experiments. Assemble input files for all Canadian CANDU's. Address program quality assurance.

6.1.2 Crack Initiation and Growth from Hydride Blisters

Determine criteria for initiation and growth of cracks from blisters to pressure tube rupture.

Carry out two tests of blister growth to pressure tube leakage or rupture using sections of pressurized tube. Complete analysis of small specimen fracture tests.

6.1.3 Crack Initiation

To understand the crack initiation process in order to provide accurate prediction of pressure tube performance for operations in which delayed hydride cracking may be important.

1. Metallography on thermally cycled zero clearance rolled joint to determine the cracking resistance and the type of hydride distribution.

2. To complete the analysis on the interaction between DHC and fatigue. In particular, the effects of load ratio, radial hydride, irradiation, and constant load will be examined.

3. To continue the four point bend and cantilever beam tests to produce crack initiation time data. Threshold stress intensity value for DHC from cracked blisters will also be obtained.

4. To correlate the critical stress state parameters that cause crack initiation with the type of hydride distribution.

6.1.4 Crack Growth

To evaluate the effects of metallurgical and operating parameters on DHC velocity and provide more crack growth data on pressure tubes at reactor operating temperature and thermal cycles. Parametric study of crack tunneling under uniaxial and biaxial loading conditions. Determine effects of continuous hydrogen ingress on DHC behaviour at reactor operating temperature.

6.2 Hydride Morphology

Assess the role of residual grain-interaction stresses on hydride morphology in Zr-2.5% Nb alloys.

Characterization of internal stresses will be done by neutron diffraction technique and optical and electron metallographic techniques will be used to study hydride morphology.

6.3 Nondestructive Evaluation of Hydrogen in Pressure Tubes

To develop a technique for the in-situ nondestructive evaluation of hydrogen (deuterium) in zirconium pressure tubes.

6.3.1 Proposal for 1989/90

A major portion of the work will focus upon the construction and testing of a prototype measuring system with retractable heaters and probes. Preliminary tests will be performed on an nonirradiated pressure tube with axial hydrogen concentration gradients present. Test will then proceed to irradiated pressure tubes. The prototype will then be prepared for in-reactor tests.

6.4 Corrosion Fatigue Boiler Tube Failures in Waterwalls and Economizers - EPRI Project RP 1890-5

This project will be on hold for most the year due to funding restrictions imposed by EPRI on the overall study. The facility will be used to perform the initial tests of the test matrix. The facility will be maintained in operational conditions as EPRI will again fund this study in 1990.

7.0 DEFORMATION MECHANISMS UNIT

7.1 Analysis of In-Service Deformation Behaviour of Fuel Channels

The existing database of power reactor deformation and operating data will be assessed, including: elongation data, diametral and sag data for PIP and ISI channels, contact data, fast flux data, temperature profiles. Deficiencies will be identified, and work continued on upgrading and maintaining them in a form available to COG participants (Task continued from 1988/89).

The study of contact development will be extended to lower powered channels, and CANDU 600 operating conditions.

CDEPTH Version 6, will be tested for a variety of conditions. The assumptions used in CDEPTH will be assessed and work started on verification of some aspects (eg, contact stiffness).

Crystallographic textures of offcuts of Bruce 2 tubes exhibiting high and low elongation rates will be measured using x-ray diffraction and correlated with deformation behaviour (task postponed from 1988/89).

7.2 High Fluence Irradiation Effects in Zr-2.5 Nb Pressure Tubes

Determine the effects of microstructure, temperature and fast neutron fluence on the irradiation deformation behaviour of standard and modified Zr-2.5% Nb pressure tube material. Extend the data base for both creep and growth to end-of-life fluences.

Continue irradiation of 40 growth specimens at 280 and 310°C in Dido. Investigate the microstructure of surveillance tube and irradiation growth specimens by analytical and transmission electron microscopy. Evaluate differences in growth of surveillance tube specimens and growth specimens irradiated without stress from zero fluence. Evaluate the effect of temperature on the steady-state growth rate. WP 3515.

Perform first measurements of seven creep and fourty-two growth specimens irradiated in Osiris (to a fluence of about $1x10^{25}$ n/m^2, E>1MeV). Measure dimensional changes in compact tension specimens irradiated in Osiris for fracture toughness assessment. Analyse neutron diffraction measurements of residual stresses and grain ODF's of growth specimen materials. WP3515/3324

Benefit: Provide information on the deformation behaviour of pressure tubes in advance of the lead power reactor to assure continued satisfactory performance. Provide input into both empirical and fundamental design equations for pressure tube deformation to allow accurate prediction of potential deformation related problems (eg, contact and contact spreading).

7.3 Evaluation of Power Reactor Fast Fluxes

Obtain quantitative correlations between the fast fluxes experienced by power reactor components and by small specimens exposed in test reactors.

1. Irradiate one "fixed element" bundle containing flux and displacement damage monitors in a low power position in Bruce A.
2. Complete tooling and procedure development for "demountable" bundle.
3. Irradiate one "fixed element" bundle containing stress relaxation, growth, tensile and delayed hydrogen cracking specimens in a Bundle #8 position in Bruce A.
4. Analyze displacement damage and flux monitors, and test specimens from first two bundles.
5. Commence irradiation of second "fixed element" bundle, containing tensile and DHC specimens in Bundle #8 position in Bruce A.

7.4 Advanced Carrier Bundle

Assess feasibility of carrier bundles for high exposure irradiations of pressure tube materials in power reactors.

1. Preliminary design study to assess fuel handling system capability and establish costs of modifications.

2. Preliminary design study of the carrier bundle and the costs of qualification program.

3. Assess possibilities and costs of licensing an LEU bundle design.

4. Develop preliminary program of irradiations.

5. Assess operational difficulties with stations.

6. Prepare recommendation to technical committee.

7.5 Fuel Clad Oxidation

Extend the available data base for biaxial deformation behaviour of Zr-4 in air to steam environments. Refine the experimental procedure developed for heating Zr-4 to elevated temperatures in steam and carry out tests needed to assess fuel cladding failure to to Be-braze assisted cracking at high temperatures in steam.

Carry out a test program which will increase the available data base for the biaxial deformation behaviour of Zr-4 fuel cladding in steam over the temperature range 673-1123 K. Perform mechanical tests and metallurgical examinations to obtain the relevant materials data. Use the new data to update and/or modify existing criteria for failure and "handling" of partially oxidized and deformed (strained) fuel cladding subjected to degraded cooling conditions.

Refine the test procedure for heating Zr-4 fuel cladding to temperatures in excess of 1273 K in steam. Carry out tests required to quantify the role of the Be-braze assisted cracking mechanism to fuel cladding failure in steam at elevated temperatures.

7.6 Pressure Tube Development

Further work to understand and/or correct the cracking of TG3 R1 pressure tubes in the cold draw stage of production will be performed. The initial program will have three extrusions cold drawn in the passes to about 40% wall reduction with the use of low angle dies. The use of such dies was recommended by Prof. B. Avitzur as a solution to the shear crack problem encountered in the 1988 production of TG3 R1 pressure tubes. A development program will also be initiated to study the workability of Zr-2.5 Wt% Nb with the purpose of providing information on how production routes could be modified without an increase in the reject route from process induced defects.

7.7 Support for Thermal Plants

The discovery of creep cracking in the main steam line at Lakeview has resulted in extensive plant investigation. In support of this problem creep tests will be performed on material from the Lakeview main steam line. The work will concentrate on accelerated tests to establish if the creep failure can be reproduced in the laboratory. From these tests the residual life of the material will be evaluated. The studies will involve staff from CPS and the Metallurgy Section.

8.0 SEM PROGRAMS

The JEOL 840A scanning electron microscope will continue to provide a service to other Sections in the Division. However, the work programs accepted for the SEM will have to require the capabilities of the 840A instrument and the priority will be given to long-term projects. One area of added work is a Director's Fund project related to the surface modification of heat exchanger materials.

Approved by:

J. Brown
Manager
Metallurgical Research dept

Prepared by:

R.G. Fleck
Supervising Engineer
Materials Integrity Section

REPORTS

88-35-K	Materials Integrity Section: A Review of 1987 and Proposals for 1988. R.G. Fleck
88-58-H CANDEV 88-52	Transmission Electron Microscopy Studies in Support of COG Research Programs. R.A. Holt and Mike Griffiths (AECL)
88-109-P CANDEV 88-69	Creepsag of Zr-2.5% Nb Pressure Tubes in CANDU Reactors Pressure Tubes in CANDU Reactors N. Badie and J. Tadros
88-129-P CANDEV 88-79	Crack Initiation in Zr-2.5 Wt% Nb Pressure Tube Material under Increased Hydro Conditions. W.K. Lee
88-154-K	Tensile Properties of AW and PWHT PN-229 Weld Metals in the Temperature 20-350°C under Constant Applied Stress E.T.C. Ho and M.J. McGraw
88-236-H CANDEV 88-142	The Effect of Temperature on the Irradiation Growth of Cold-Worked Zr-2.5 wt% Nb. R.A. Holt and R.G. Fleck
88-259-P CANDEV 88-159	Effect of Spacer Location and Operating Conditions on Contact Spreading N. Badie and S. Unterbergs
88-324-K	Probabilistic Assessment of Pickering Unit 4 Cores for Pressure Tube Cracking Due to Hydride Blister Formation M. Leger, D.V. Leemans and T.P. Byrne
M88-5-K	Evaluation of the JVK High Temperature Extensometer Developed at AECL-CRNL E.T.C. Ho and M.J. McGraw
M88-26-K	Overview of CM^2 (Centre for Microscopic Characterization of Materials S. Sandloehken
M88-25-K	A Test Facility for Oxidation Studies of Zircaloy-4 Fuel Cladding Samples in a Steam Environment E.T.C. Ho and A. Donner
M88-30-K	Tensile Properties of Some Current Zr-2.5 wt% Nb Pressure Tube Material Made to the Task Group Three Specifications E.T.C. Ho and M.J. McGraw

REPORTS (Cont'd)

M88-47-K — Effects of Temperature and Load Maneuvering on DHC Behaviour on Zr-2.5 Wt% Nb Pressure Tube
G.K. Shek and H. Seahra

M88-85-K — Tensile Properties of TG3 Route 1 Tubes at Different Cold Work Stages
G.K. Shek and H. Seahra

M88-96-K — International Conference on Environment-Induced Cracking of Metals - Trip Report
E.T.C. Ho

PRESENTATIONS/PUBLICATIONS

"The β to α - Transformation in a Zr-2.5 Wt% Nb Alloy", March 14, 1988, ACTA Metallurgica.
V. Perovic and G.C. Weatherly

"Sag of Zr-2.5% Nb Pressure Tubes", at 9th Annual Conference of the Canada Nuclear Society, Winnipeg, June 15, 1988.
N. Badie, R.A. Holt, C.W. Schulte, R.G. Sauv

"Effects of Hydride Morphology on Zr-2.5 Nb Fracture Toughness", at VIII International Conference on Zirconium in the Nuclear Industry, San Diego, June 20, 1988. ASTM Special Technical Publication.
A.C. Wallace, O.E. Lepik and G.K. Shek

"Effects of Loading and Thermal Maneuvers on Delayed Hydride Cracking in Zr-2.5 Wt% Nb Alloys", at VIII International Conference on Zirconium in the Nuclear Industry, San Diego, June 20, 1988. ASTM Special Technical Publication.
G.K. Shek and D.B. Graham

"Growth Fracture and Nondestructive Evaluation of Hydride Blisters in Zr-2.5 Wt% Nb Pressure Tubes", at VIII International Conference on Zirconium in the Nuclear Industry, San Diego, June 20, 1988. ASTM Special Technical Publication.
M. Leger, A.C. Wallace, G.D. Moan and N.J. Watson

"The Effect of Temperature on the Irradiation Growth of Cold-Worked Zr-2.5% Nb, at VIII International Conference on Zirconium in the Nuclear Industry, San Diego, June 20, 1988. ASTM Special Technical Publication.
R.A. Holt and R.G. Fleck

J. Nuclear Materials 158 (1988) 49, November 1988.
T. Laursen, M. Leger and J.L. Whitton

J. Nuclear Materials 159 (1988) 310, December 1988
R.A. Holt

J. Nuclear Materials 159 (1988) 75, December 1988
R.G. Fleck, R.A. Holt, V. Perovic & J. Tadros

J. Nuclear Materials 159 (1988) 225, December 1988
A.R. Causey, C.H. Woo, R.A. Holt

CONFERENCES AND TECHNICAL MEETINGS

Visit to CANDU OPs to discuss orientation of pressure tubes in Darlington, February 19, 1988.
R.A. Holt and R.G. Fleck

Visit to Chalk River, Ontario to discuss COG programs, Feb 2-3, 1988.
R.A. Holt

Visit to Bruce NGS A to discuss carrier bundle experiments with station staff, March 23, 1988.
R.A. Holt

Meeting with B.A. Cheadle at AECL-CRNL, April 26-17, 1988.
R.A. Holt

Meeting at AECL-RC, Chalk River, Ontario to discuss crack initiation and growth programs, May 15-16, 1988.
W.K. Lee and G.K. Shek

Meeting with C.H. Woo, I Ritchie an R. Dutton, AECL-WNRE, Winnipeg, May 24-26, 1988.
R.A. Holt

Attend the Metal Physics Conference, Kingston, Ontario, June 8-10, 1988.
M. Leger

Visit UKAEA and CEA, France and UK, June 8-11, 1988
R.A. Holt

Attended Ninth Annual Conference of the Canadian Nuclear Society, Winnipeg, Manitoba, June 12-15, 1988.
N. Badie

Attended Eighth International Conference on Zirconium in the Nuclear Industry, Sand Diego, California, June 18-24, 1988.
G.K. Shek, M. Leger, R.A. Holt

Visit AECL-CRNL, Chalk River, Ontario to discuss experimental technique to measure delayed hydride crack velocity, June 29, 1988.
G.K. Shek

Visit Nu-Tech, Arnprior, Ontario to discuss TG3 Route 1 tube production problem, June 30, 1988.
G.K. Shek

Visit to AECL-CRNL, Chalk River to discuss crack tunnelling and fracture toughness methodology, August 9, 1988.
G.K. Shek, M. Leger

CONFERENCES AND TECHNICAL MEETINGS (Cont'd)

Visit to Nu-Tech, Arnprior, Ontario to observe drawing of production TG3 pressure tubes and discuss preparation problems, August 16, 1988
R.A. Holt

Ninth European Congress on Electron Microscopy, York, England, September 4-9, 1988.
V. Perovic

Visit to AECL-CRNL, Chalk River to discuss delayed hydride cracking at CRNL, Chalk River with Prof. E. Smith, September 16, 1988.
W.K. Lee, G.K. Shek

Attend meeting on Probabilistic approaches to leak-before-break at WNRE, September 20, 1988.
M. Leger

Attend meeting at Nutech with S.A. Aldridge, B.A. Cheadle and G. Moan to discuss TG3 preparation route and possible source of problems. September 22, 1988.
R.A. Holt and R. Fleck

Visit to AECL-RC, Chalk River to discuss COG projects, October 6, 1988.
V. Perovic

Visit to AECL-RC, Chalk River to discuss COG projects, December 12-14, 1988.
R.A. Holt

Visit to AECL-RC, Chalk River to discuss COG projects, December 13, 1988.
V. Perovic

Visit to CANMET - Ottawa to discuss TEM, December 14, 1988.
V. Perovic